The Dissertation Committee for Mingzhe Zhao Certifies that this is the approved version of the following dissertation:

Regulation of Arabidopsis Trichome Patterning and Anthocyanin Biosynthesis by the TTG1-bHLH-MYB Complex

Committee:

Alan M Lloyd, Supervisor

Robert K. Jansen

Paul Macdonald

Terry O'Halloran

Stanley J. Roux

Regulation of Arabidopsis Trichome Patterning and Anthocyanin Biosynthesis by the TTG1-bHLH-MYB Complex

by

Mingzhe Zhao, B.S. M.S.

Dissertation

Presented to the Faculty of the Graduate School of

The University of Texas at Austin

in Partial Fulfillment

of the Requirements

for the Degree of

Doctor of Philosophy

The University of Texas at Austin

August 2007

Dedication

To my beloved family and friends

For their support and inspiration

Acknowledgements

Though the following dissertation is an individual work, it could never have been completed without the help, support, guidance and effort of a lot of people. First, I would like to truly thank my mentor, Dr. Alan Lloyd, for his generous time, patience and most importantly, his understanding throughout my graduate studies at the University of Texas at Austin. His guidance and support continually encouraged me to grow as an independent thinker and experimentalist. I have also been tremendously inspired by his unique insight and unlimited passion to both science and life.

I am very grateful for having an exceptional doctoral committee and wish to thank Dr. Robert Jansen, Dr. Paul Macdonald, Dr. Terry O'Halloran and Dr. Stan Roux for their continual support and encouragement. I am especially thankful to Dr. Paul Macdonald for allowing me to use his lab and equipment for the microscopy and Western work.

I would also like to thank all of the members of the Lloyd lab, especially Vaughan Symonds, Brian Windsor, Frank Zhang, Antonio Gonzalez, Sarah Conte and Greg Hatlestad. These friends and co-workers have helped me, saved my plants and made this dissertation work possible. They have also provided for some much needed humor and entertainment in what could have otherwise been a somewhat stressful laboratory environment.

I am extremely grateful for the assistance, generosity, and advice I received from Dr. Erich Grotewold and Dr. Kengo Morohashi at the Biotechnology Center, Ohio State University. It is not often that a graduate student gets the opportunity to collaborate with such a gifted team of researchers. Our collaboration has truly broadened my view of science.

I owe a special note of gratitude to the people at the core facility: John Mendenhall and Dr. Angela Bardo for assisting me with confocal microscopy; Dwight Romanovicz for SEM; Josh Russell for image processing; Dr. Klaus D. Linse for the protein work and Cecil W. Harkey for RT-PCR.

I extend many thanks to my colleagues and friends, especially from the Fisher, Stevens, Krug, Elington and Iyer labs: Xin Chen, Erin Overstreet, Andrew Adam Roth, Nan Yan, Cuiyun Geng, Chen Zhao, Litao Yang, Jian Gu and Youzhong Guo.

Finally, I'd like to thank my family and friends: Sky Soon, Dorothy Lee, Joyce Chen, Buang Ann Tay, Anna Chen, Richard Su, Carrie Wang, William Chang, Glenn Chou and Made Setiawan for helping me keep my life in proper perspective and balance.

This research was partially funded by the National Science Foundation. I would like to thank the Institute of Cellular and Molecular Biology and the Program of Molecular Cellular Developmental Biology at UT. I extend my thanks to Barbara Welch for doing an excellent job with overseeing and managing my academic paperwork.

Regulation of Arabidopsis Trichome Patterning and Anthocyanin Biosynthesis by the TTG1-bHLH-MYB Complex

Publication No._____

Mingzhe Zhao, Ph.D.

The University of Texas at Austin, 2007

Supervisor: Alan Lloyd

A network of three classes of proteins consisting of bHLH and MYB transcription factors and a WD40 repeat protein - TRANSPARENT TESTA GLABRA1 (TTG1) act in concert to activate trichome initiation and patterning in *Arabidopsis*. These proteins also regulate the flavonoid-based pigment biosynthetic pathway in almost all higher plants including *Arabidopsis*. Using TTG1-YFP translational fusions, I show that TTG1 is expressed ubiquitously in *Arabidopsis* leaves and is preferentially localized in the nuclei of trichomes at all developmental stages. Using conditional transgenic alleles I demonstrate that TTG1 directly regulates the same genes as GL3. In vivo binding of GL3, GL1 and TTG1 to the promoters of GL2, TTG2, CPC and ETC1 establishes that these genes are major transcriptional targets for the TTG1-bHLH-MYB regulatory complex. By co-precipitation, I confirm that TTG1 interacts with the GL3 (bHLH) and GL1 (Myb) proteins in vivo, forming a complex. The loss of members of the TTG1 complex through mutation, affects the subcellular distribution of other complex members. Using particle bombardment, I show that TTG1, GL3, GL1 and GL2 do not move

between adjacent epidermal cells while CPC does move to neighboring cells. These data support a model for the TTG1 complex directly regulating activators and repressors and the movement of repressors to affect trichome patterning on the *Arabidopsis* leaf.

In addition, I also show that GL3 is recruited to its own promoter in a GL1-independent manner, which results in decreased GL3 expression, suggesting the presence of a GL3 negative auto-regulatory loop.

Expression studies using GL3-GR (GL3-glucocorticoid receptor) and TTG1-GR fusions reveal direct regulation of the late anthocyanin biosynthetic genes, but not of early biosynthetic genes. Taken together, our results provide insights on the molecular mechanisms by which the combinatorial TTG1-bHLH-MYB regulatory complexes activate and repress both developmental and biosynthetic pathways in *Arabidopsis*.

Table of Contents

List of Figures

Chapter 1: General Introduction

Plant development

The development of a plant from a single-celled zygote into a complex multi-cellular organism can be divided into stages such as embryogenesis, seed germination, shoots and roots elongation and branching and flowering. For ages, people have been trying to learn the secrets behind these development events.

Growth and differentiation are two interrelated processes defining plant development. During differentiation, uniform plant cells differentiate into a diverse array of specialized cells largely by making specific cell-fate decisions. Once the cell fate is determined the cell will grow into a mature cell of certain size by mechanisms such as expansion and then thickening the walls. Because the cell-fate determination provides "starting points" for the development of certain tissues, the understanding of cell-fate determination is considered to be fundamental to understanding plant development.

Arabidopsis thaliana as a model plant

Arabidopsis is a small flowering plant in the mustard family. It has a century-long history of being the ideal model plant in plant biology because of its small size, short generation time, and up to ten thousand seeds produced by a single plant. *Arabidopsis* is easy to grow year round in the greenhouse with simple watering and fertilization requirements. In the early years, *Arabidopsis* was used mostly in genetics laboratories for classical genetic studies. A large number of mutants, defective in a great variety of processes, have been generated by chemical, radioactive, and insertional mutagenesis, leading to the identification of thousands of genes with important biological functions. The recent fast growth of plant biotechnology is requiring basic information about plant

biology more than ever. The ambition to bioengineer agriculturally important plants such as rice, corn and cotton draws even more attention to the model plant *Arabidopsis*. By the year 2000, the completion of sequencing the whole *Arabidopsis* genome (5 chromosomes, 125Mb) was a milestone in plant biology (Lin *et al*. 1999; Mayer *et al*. 1999; Salanoubat *et al*. 2000; Tabata *et al*. 2000; Theologis *et al*. 2000). It is a huge achievement in the efforts to understand plant life at the genetic and molecular level and makes it possible to create valuable plants for agriculture, medicine, and energy. Since then, many molecular biology techniques have been developed, in particular for *Arabidopsis*. The utilization of these techniques has generated constant waves of interest and contributed powerful information in every field of plant biology especially in plant developmental biology. *Arabidopsis* has become a widely accepted model plant for understanding mechanisms underlying developmental processes such as cell fate determination and cell patterning.

Arabidopsis thaliana epidermis and TTG1-dependent pathways

In order to study cell-fate determination, a system is needed in which I should be able to easily monitor and manipulate specific single-cell fate switches. Then I could pose questions and hypotheses about development problems and test these hypotheses at the molecular and whole plant levels. Studies on the regulation of cell fate and function on the plant epidermis continue to provide important insights into how plant cells are organized, how patterning develops, and how developmental and biochemical pathways interact. The *Arabidopsis* epidermis is the "skin" (outermost cell layer) of *Arabidopsis* body. Because it is the cell layer through which gas exchanges, all light flows and nutrients must pass, it is particularly important to understand how this layer functions.

The *Arabidopsis* epidermis is comprised of several distinct cell types (Ramsay and Glover 2005), in which genes are very tightly regulated to ensure the appropriate cell identities and patterning. *Transparent Testa Glabra1* (*TTG1*) locus functions to regulate many seemingly disparate epidermal pathways, which are also referred as TTG1-dependent pathways. These pathways include trichome initiation, anthocyanin pigment production, seed coat tannin production, seed coat mucilage cell differentiation, and root hair and nonhair cell fate. Mutations in *TTG1* cause pleiotropic phenotypes such as loss of trichome on leaves and stems, extra root hairs in the non-root hair position and loss of pigment and mucilage production (Koornneef, 1981; Galway *et al*. 1994).

TTG1-WD40 protein

After a chromosome walk lasting for over six years, the *TTG1* locus was isolated and reported to encode a protein containing WD-repeats homologous to repeats found in mammalian heterotrimeric G-protein B subunits (Walker *et al*. 1999). WD40 proteins are a propeller protein family with from four to sixteen tandemly repeated WD40 motifs. WD-repeats are reported to be involved in protein-protein interactions and intramolecular folding. Although the first WD repeat containing protein identified was a G-protein beta subunit, most WD proteins are not in this class (Neer *et al*. 1994). All bona-fide G-protein beta subunits reported to date contain seven copies of the WD40 motif. TTG1 and An11 (a petunia WD40 protein which is highly similar to TTG1 and complements the *ttg1* mutation (not shown)) have only five WD40 repeats and our near-neighbor phylogenetic analysis does not place them particularly close to the G-protein beta subunits, making it unlikely that they are in this class. Included in the WD repeat group are several from plants including COP1 (Deng *et al*. 1992) and PRL1 (Nemeth *et al*. 1998) as well as other proteins, such as ZGB1 and AGB1, which look like much better

candidates for G-protein beta subunits (Weiss *et al*. 1994). COP1 is reported to have five WD repeats and it interacts with HY5, a bZIP transcription factor, through this domain (Torii *et al*. 1998). PRL1 has seven repeats and interacts with ATHKAP2, a nuclear import receptor (Nemeth *et al*. 1998).

TTG1 functions are still unknown. Due to the fact that the TTG1 sequence contains no recognizable nuclear localization signal or DNA binding motif or transcriptional activation domain, it seems probable that TTG1 does not directly act as a transcription factor. Earlier work on the An11 has reported a role for this WD40 motif protein in the regulation of anthocyanin production. In the case of Petunia, the An11/WD40 mutation is partially suppressed by overexpression of An2, a myb element in the C1/GL1 class of transcription factors, but not by expression of An1, a basic-helix-loop-helix (bHLH) class protein (de Vetten *et al*. 1997). This is in contrast to *Arabidopsis* where overexpression of bHLH proteins, R, GL3 and EGL3 but not myb proteins, either C1, GL1, MIXTA or CotMYBA, suppresses the *ttg1* mutation (Lloyd *et al*. 1992; Galway *et al*. 1994; Lloyd *et al*. 1994; Payne *et al*. 1999). An11 was proposed to be involved in a signal transduction cascade that leads to the post-translational modification or subcellular localization of An2, the myb element. Therefore, TTG1 might function through affecting the *Arabidopsis* bHLH factors such as GL3/EGL3. In this thesis, the findings on TTG1 function in *Arabidopsis* shed light on understanding other WD repeat proteins in other species.

The combinatorial regulatory complex: WD-bHLH-MYB

The TTG1-dependent pathways are regulated by three classes of proteins consisting of bHLH and MYB transcription factors and TTG1, which are proposed to form a combinatorial regulatory complex: WD-bHLH-myb. Work by our group and a

host of others has genetically identified and cloned many members of the TTG1 complex. TTG1 (Koornneef *et al*. 1982; Walker *et al*. 1999) is the single WD repeat containing protein in the complex. The bHLHs in the complex are GL3 and EGL3 (Payne *et al*. 2000; Zhang *et al*. 2003), TDL5/Atmyc1 (identified by our lab), and TT8 (Nesi *et al*. 2000). The R2R3 myb elements are more numerous and include, GL1 (Oppenheimer *et al*. 1991), WER (Lee & Schiefelbein 1999), TT2 (Nesi *et al*. 2001), the PAP1/2, Myb113/114 4-member subgroup (Borevitz *et al*. 2000; our lab), and Myb5. There is also a family of single repeat, R3 mybs that have no transcriptional activation domain and these appear to all be involved in root hair and trichome near neighbor signaling. Different transcription factor combinations can specify the state of the pathway regulated (Figure 1.1).

Arabidopsis Trichome development

Trichome development is one of the most well studied *Arabidopsis* epidermal development processes. *Arabidopsis* trichomes are large cells protruding from the epidermis of leaves and stems. Most mature trichomes could grow up to 200 um long and are surrounded by 8 to 12 basal cells. They are easily visible and accessible at low magnifications on microscopes. Trichomes are believed to protect plants from insect herbivores, UV light and loss of water by transpiration. The trichome pathway seems to cross-talk with other pathways. For example, analysis on GA (gibberellic acid) mutants *ga1-3* and *spy-5* have indicated that GAs can induce trichomes (Perazza *et al*. 1998). Jasmonic acid and salicylic acid have also proved to be able to affect trichome production (Traw and Bergelson 2003). Furthermore, mutations in UPL3, an ubiquitin ligase, can cause extra branches in leaf trichomes (Downes *et al*. 2003). These studies have suggested that hormone signaling and protein degradation may share the same regulators

with trichome development at some point. However these regulators remain largely uncharacterized.

Mature trichomes are present at the tip of the young leaf, while towards the base of the leaf there is a progression of trichomes at progressively earlier developmental stages. Six phases characterize trichome development (Szymanski *et al*. 1998), starting with the radial expansion of an epidermal cell (trichome initial) and concluding with the formation of a mature trichome, characterized by the presence of a stalk with 2-4 branches and a 32C DNA content (Hulskamp *et al*., 1994). Trichome mutants have been created either by chemical, insertion or radiation mutagenesis. Over 30 genes controlling various aspects of trichome initiation, spacing, size and morphology (Schellmann and Hulskamp, 2005).

Trichomes initiate and develop on young leaves in a regular spacing pattern (Larkin *et al*. 1997; Marks 1997; Hulskamp and Schnittger 1998; Hulskamp *et al*. 1999). This trichome patterning is not random or dependent on other cell types or position on the leaf, but thought to be generated *de novo* by intercellular communication (Larkin *et al*. 1996; Schnittger *et al*. 1999). It is postulated that inhibitors which are activated by self-enhanced activators can move between cells to mediate the competition between equivalent cells thereby resulting in the pattern formation (Larkin *et al*. 2003; Pesch and Hulskamp 2004).

Current model for the trichome initiation and patterning

Years of genetic and molecular studies have enabled the identification of components of this trichome patterning machinery (Fig. 1.2). Three classes of interacting regulators including the R2R3-MYB transcription factor, GL1 (Oppenheimer *et al*. 1991), the basic helix-loop-helix (bHLH) proteins, GL3/EGL3 (Payne *et al*. 2000; Zhang

et al. 2003) and the WD40 repeat protein, TTG1 (Walker *et al*. 1999) are postulated to form a combinatorial regulatory complex. Support for this complex comes from yeast two-hybrid studies showing that TTG1 and GL1 physically interact with GL3/EGL3 but not with each other (Payne *et al*. 2000; Zhang *et al*. 2003). This TTG1-bHLH-GL1 regulatory complex is believed to activate the expression of *GLABRA2 (GL2)* (Szymanski *et al*. 1998) and thereby regulates trichome development. *GL2* encodes a homeo-domain-Zip (HD-Zip) transcription factor and is required for normal trichome development (Rerie *et al*. 1994). Some levels of GL2 overexpression can result in trichome clusters, implicating this HD-Zip factor in the regulation of trichome spacing (Ohashi *et al*. 2002). GL2 is also required for seed coat mucilage cell differentiation and root hair patterning (Di Cristina *et al*. 1996; Masucci *et al*. 1996). In roots, GL2 promotes non-root hair cell fates by directly repressing a Phospholipase D 1 gene (Ohashi *et al*. 2003) that may be involved in signal transduction.

To date, a group of at least four homologous single MYB proteins TRIPTYCHON (TRY) (Schellmann *et al*. 2002), CAPRICE (CPC) (Wada *et al*. 1997) and ENHANCER OF TRY and CPC1 and 2 (ETC1 and 2) (Kirik *et al*. 2004a; Kirik *et al*. 2004b) have been identified as negative regulators of trichome initiation/patterning. The *try cpc* double and the *try cpc etc1* triple mutants (Schellmann *et al*. 2002; Kirik *et al*. 2004a) showed a greatly enhanced "clustered-trichome" phenotype, indicating that the lateral inhibition was disrupted. These inhibitory proteins contain no recognizable transcription activation domain. Therefore, they could work as negative transcriptional regulators. Protein interaction analysis in yeast has suggested that TRY or CPC would interrupt the functionality of the "activating" TTG1-bHLH-GL1 complex by competitive interaction with the bHLH (Esch *et al*. 2003; Zhang *et al*. 2003). Additionally, the individual members of this inhibitory protein family may function differently. There is

evidence that TRY might be more important in short-range inhibition while CPC and particularly ETC1 may be important for long-range inhibition (Schellmann *et al*. 2002; Kirik *et al*. 2004a).

As I described above, the identification of these positive and negative trichome regulators has laid out an excellent foundation for understanding trichome patterning. However, a large amount of the data elucidating the molecular mechanism played by these regulators is either indirect or obtained from another similar pathway - root hair patterning. For instance, evidence for the existence of the TTG1-bHLH-MYB complex is completely based on protein interaction studies in yeast (Payne *et al*. 2000; Zhang *et al*. 2003). Furthermore, the only evidence so far demonstrating the ability of a single MYB inhibitor to move between cells is that CPC-GFP fusion protein is detected both in the trichoblasts and in the atrichoblasts in roots when it is only transcribed in hairless cells (Wada *et al*. 2002). More importantly, the regulatory events triggered by the TTG1-bHLH-GL1 active complex mostly remain unknown, except that the expression of CPC in the root epidermis is GL3/EGL3 dependent (Bernhardt *et al*. 2005) and directly regulated by Werewolf (WER) (Lee and Schiefelbein 2002; Koshino-Kimura *et al*. 2005; Ryu *et al*. 2005), a GL1 equivalent protein in root hair patterning (Lee and Schiefelbein 2001). In this thesis, molecular studies have been performed aiming to directly test and refine the regulation mechanism during trichome initiation and patterning.

Figure 1.1: TTG1-bHLH-Myb combinatorial complex model for pleiotropic regulation of epidermal pathways.

Heavy arrows indicate how the various complex member proteins interact (not all interactions are included) and the pathways regulated are indicated with light arrows.

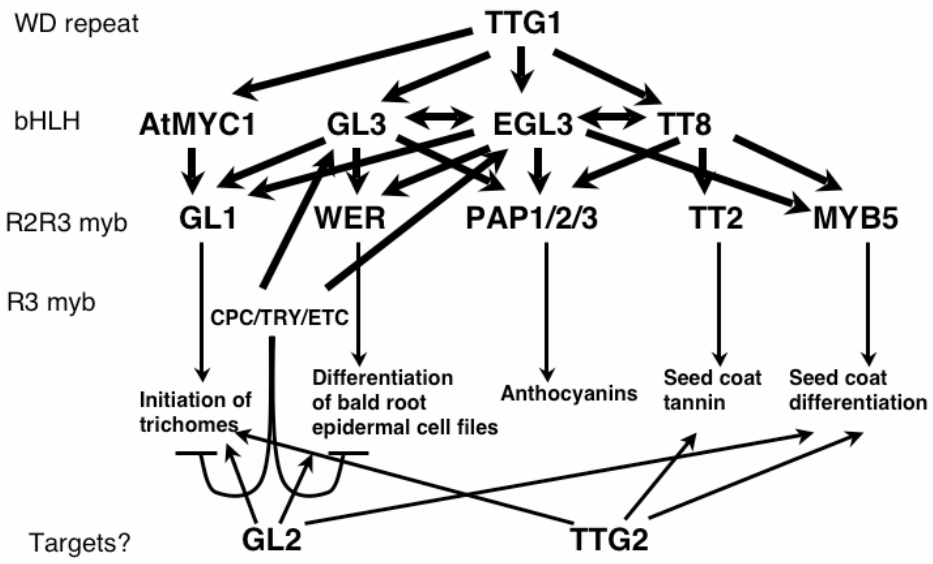
WD repeat
TTG1
bHLH
AtMYC1
GL3
EGL3
TT8
R2R3 myb
GL1
WER
PAP1/2/3
TT2
MYB5
R3 myb
CPC/TRY/ETC
Initiation of trichomes
Differentiation of bald root epidermal cell files
Anthocyanins
Seed coat tannin
Seed coat differentiation
Targets?
GL2
TTG2

Figure 1.2: Current model for *Arabidopsis* trichome initiation and patterning.

Regulators of trichome fate are depicted in green shades, activator is in yellow and inhibitors are in red. Arrows indicate transcriptional activation. In trichome cells the inhibitors are activated by the activating complex and move into neighboring cells, where they block the activity of the activating complex thereby inhibiting trichome fate.

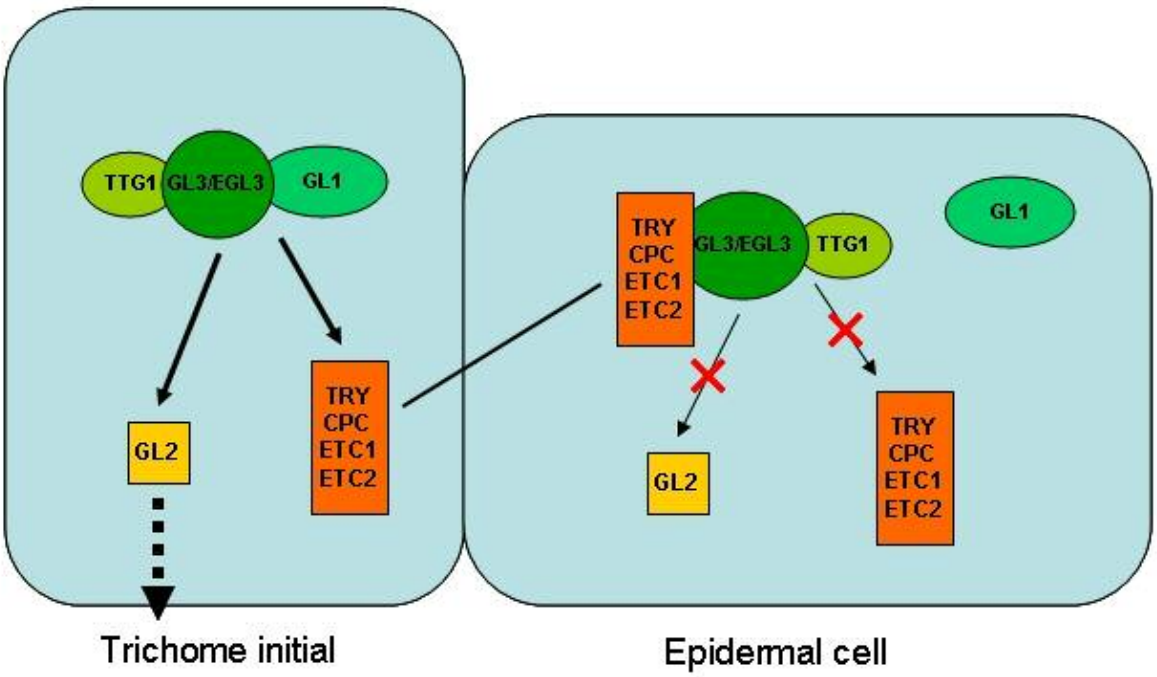

Chapter 2: Participation of GL3 in Trichome Initiation Regulatory Events

INTRODUCTION:

bHLH transcription factors GL3 and EGL3 are key regulators of trichome development. They are highly similar in their physical sequences. GL3 protein is 637 amino acids long with a bHLH domain close to the carboxy terminus. EGL3 is 39 amino acids shorter and shares 75% amino acid identity with GL3 throughout its whole sequence.

While *gl1* and *ttg1* mutants are mostly glabrous, mutations in *gl3* have only a modest effect, primarily affecting branching, DNA endoreduplication and trichoblast size (Hulskamp *et al*., 1994; Payne *et al*., 2000). In contrast, *egl3* plants have no obvious trichome defect, but *gl3 egl3* double mutants show a completely glabrous phenotype (Zhang *et al*., 2003). The *gl3 egl3* double mutant also shows other phenotypes including disrupted root hair patterning, less shoot anthocyanin pigment production and less seed coat mucilage than wild type plants. In the *gl3 egl3 tt8* triple mutant, anthocyanins and seed coat mucilage disappear. These results demonstrate that GL3 and EGL3 function in multiple epidermal pathways.

Expression of both GL3 and EGL3 is low in the developing epidermis of young leaves, increases in initiating and young trichomes and drops in mature trichomes and pavement cells of mature leaves (Zhang *et al*., 2003). This is similar to *GL1* and consistent with their participation in the selection of protodermal cells to the trichome pathway (Larkin *et al*., 1993). Overexpression of GL3 or EGL3 would partially suppress the *ttg1* mutant to different levels, however co-overexpressing GL3 and EGL3 strongly

suppresses *ttg1* phenotypes producing supernumerary trichomes and as much or more seed coat pigment as wild type (Zhang *et al*., 2003).

Although *GL3* and *EGL3* are very similar, evidence suggests that they are functionally partially different. For instance, overexpression of EGL3 represses mucilage defect in the *ttg1* mutant while overexpression of GL3 does not (Zhang *et al*., 2003). On the other hand, overexpression of GL3 is a better trichome repressor in the *ttg1* mutant than overexpression of EGL3 (Zhang *et al*., 2003). Detailed function analysis of bHLHs would enable us understand better about how the duplication or divergence of these developmental regulators drives morphological changes from an evolutionary perspective.

Using a combination of post-translationally controlled GL3-glucocorticoid receptor fusions (GL3-GR), experiments were directed at testing two specific hypotheses: 1) GL3 directly regulates specific trichome regulatory loci and 2) the regulatory function of the GL3 is dependent on GL1. Our results show that some but not all of the trichome initiation genes are direct targets of GL3. Our results also uncover two GL3 regulatory mechanisms, one of which is GL1-dependent and the other GL1-independent. I also exposed an unexpected binding of GL3 to its own promoter, suggesting the potential for a GL3 auto-regulatory feedback. Together, these findings provide novel insights into the regulatory motifs participating in the initiation of trichome formation.

MATERIAL AND METHODS

Arabidopsis strains and Plant Growth

The mutant alleles used in this study have been described: *gl3-2* and *gl3 egl3* are in the *Ler* background (Payne *et al*., 2000; Zhang *et al*., 2003); *gl1* is in the *Col* genetic

background (). The *gl3 egl3* mutant was transformed with pGL3::GL3-YFP (Bernhardt *et al*. 2005) to create *gl3 egl3*/pGL3::GL3-YFP. Transgenic plant *gl3-2/* pGL3::GL3-YFP (Bernhardt *et al*. 2005) was crossed to *gl1* mutants. Seeds from crossed F1 plants which were *gl1* mutant-like and kanamycin resistant were collected and screened for homozygous *gl1*/pGL3::GL3-YFP.

To select for transgenes, *Arabidopsis* plants were grown on soil with 100 μM BASTA (LibertyTM, AgrEvo) (*gl3 egl3*/p35S::GL3-GR) or MS media supplemented with 50 mg/l kanamycin (*gl3 egl3*/pGL3::GL3-YFP, *gl1*/pGL3::GL3-YFP) at 22ºC, under a photoperiod of 16 hours of light and 8 hours dark, unless otherwise indicated.

Description of GL3-GR Fusion Constructs

To construct the GL3-GR translational fusion clones, pD2L-2 (Payne *et al*., 2000) was modified as described (Bernhardt *et al*., 2005) to provide a *GL3* promoter and coding region genomic clone (pGL3::GL3) with the stop codon removed and replaced by *Sac*I and *Sal*I restriction sites. The GR-coding region was amplified from pRGR (Lloyd *et al*., 1994) and ligated in-frame to the GL3 3' end using the *Sac*I and *Sal*I sites. A *Bam*HI fragment from this vector, containing the entire pGL3::GL3-GR fusion, was subcloned into the *Bgl*II site of the T-DNA vector pAL47 (Lloyd and Davis, 1994) to make pGL3::GL3-GR containing GL3-GR under native control. A fragment containing the entire GL3-GR fusion, from the start GL3 codon to the GR stop codon, plus Gateway recombination sequences on both ends, was amplified from pGL3::GL3-GR and recombined into the Gateway site of the vector pDonor222 (Invitrogen) to create pGWGL3GR. pGWGL3GR was recombined with pB7WG2 (Karimi *et al*., 2002) to make p35S::GL3-GR containing GL3-GR under *CaMV35S* control.

Optical and Scanning Electron Microscopy (SEM)

Optical images were taken with a Nikon SMZ800 dissecting microscope. The *gl3 egl3* plants carrying p35S::GL3-GR were grown on soil under constant light at 22ºC for 16 days, when the 3rd and 4th leaf become visible. To induce trichomes, 20 μM DEX or 2% ethanol as mock were sprayed onto the plants once. Seedlings were collected at multiple time points between 0 - 72 hrs after the DEX treatment. For SEM experiments, plant samples were prepared and visualized essentially as described (Payne *et al*., 2000) with minor modifications. Critical-dried specimens were coated with platinum palladium in a Crossington 208 sputter coater and then visualized with a Zeiss Supra 40VP scanning electron microscope.

Gene Expression Analyses

For the *gl3 egl3*/pGL3::GL3-GR, 14 day-old seedlings were transferred from plain MS media to MS media containing 30 μM DEX or 2% ethanol (Mock). For the *gl3 egl3/*p35S::GL3-GR, 16 day-old seedlings growing on soil were sprayed with 20 μM DEX, 100 μM CHX, and 20 μM DEX + 100 μM CHX. Tissues were collected after treatment and frozen immediately in N_2 (liquid). For RT-PCR experiments, green tissues from 30 - 40 seedlings were used for each RNA extraction, following the Trizol reagent protocol. The RNA was further purified using Qiagen RNeasy®, following the manufacturer's instructions. Real-Time PCR is performed using SYBR Green chemistry (Applied Biosystems) on a 7500 Real-Time PCR System (Applied Biosystems). Primers for PCR were designed to generate unique 100-200 bp fragments. For normalization, I used ACT2 (At3g18780) or At1g13320, which is reported to be one of the best reference genes (Czechowski *et al*., 2004). Real-time PCR of test samples and the reference gene were performed at the same time, following normalization by calculation of fold ratios

between test samples and reference gene. Transcript quantification from PCR results is performed using a standard dilution series for each transcript.

Chromatin Immunoprecipitation (ChIP) Experiments

Green tissues from three-week-old plants grown on soil were washed in distilled water, and immersed in buffer A (0.4 M sucrose, 10 mM Tris-HCl pH 8.0, 1 mM EDTA, 1 mM PMSF, and 1% formaldehyde) under vacuum for 20 min. Glycine was added to 0.1 M, and incubation was continued for an additional 10 min. The plants were washed in distilled water and frozen in N_2(l). Approximately 60 mg of tissue were ground for each immunoprecipitation. The tissue was resuspended in 0.1 ml Lysis Buffer (50 mM HEPES pH7.5, 150 mM NaCl, 1 mM EDTA, 1% Triton X-100, 0.1% deoxycholate, 0.1% SDS, 1 mM PMSF, 10 mM sodium butyrate), and plant proteinase inhibitor cocktail (Sigma). DNA was sheared by sonication to approximately 300-1000 bp fragments with a main peak of 500 bp. Sonication (Sonics & Materials Inc.) was performed on ice with an amplitude of 10% using 5x15 sec pulses (5 sec between bursts). After preclearing with 40 μL of salmon sperm DNA/Protein A-agarose beads (Upstate) for 120 min at 4˚C, immunoprecipitations were performed overnight at 4˚C with either 2 μg of IgG, 1 μg of anti-GR antibody (PA1-516; Affinity BioReagents), or 1 μl of anti-GFP antibody (ab290; Abcam). After incubation, beads were washed 2 times with LNDET Buffer (0.25M LiCl, 1% NP40, 1% deoxycholate, 1 mM EDTA), and 2 times with TE buffer. The washed beads and input fraction were resuspended in Elution Buffer (1% SDS, 0.1 M $NaHCO_3$) with 1 mg/ml proteinase K, and incubated overnight at 65˚C. After crosslink reversal of the Immunoprecipitated and Input DNA (set aside from the sonication step), the DNA was purified using the PCR Purification Kit (Qiagen). Semi-quantitative PCRs was

performed under standard PCR conditions (35-38 cycles). DNA was detected using agarose gel electrophoresis, and quantified by EtdBr staining.

RESULTS

pGL3::GL3-GR is a weak transcriptional activator

In a wild-type *Arabidopsis* plant, trichome formation occurs sequentially from the tip to the base of the leaf as development progresses, making it difficult to explore the events specifically associated with trichome initiation. Because GL3/EGL3 participate both in early trichome initiation as well as during later stages (*e.g.,* during branch development), the identification of the GL3/EGL3 direct targets associated with trichome initiation can be confounded with those involved in branching and later developmental stages. To overcome these problems, I took advantage of a system to synchronize trichome initiation using *Arabidopsis gl3 egl3* plants transformed with GL3 fused to the glucocorticoid hormone receptor domain, GR.

Initially, I utilized the pGL3::GL3-GR construct, containing the *GL3* promoter and the *GL3* 3' region, which recapitulates the *in vivo GL3* expression pattern (Zhang *et al*., 2003). The *gl3 egl3*/pGL3::GL3-GR plants are glabrous, unless treated with dexamethasone (DEX), a synthetic ligand for the GR (Fig. 2.1). Several genes which have been suggested to participate in the early stages of trichome initiation (Schellmann and Hulskamp, 2005) were examined to determine whether 4 hrs of DEX treatment of *gl3 egl3*/pGL3::GL3-GR plants resulted in the activation of any of these genes. Quantitative reverse-transcriptase PCR (qRT-PCR) experiments were performed on RNA obtained from green tissues of seedlings induced for 4 hrs with DEX and compared with RNA obtained from Mock-treated plants. Of all of the trichome initiation genes tested (*GL2*,

TRY, *CPC*, *ETC1* and *ETC2),* only *GL2* showed a very modest, yet significant, induction under these conditions (not shown).

Trichome developmental genes are among the GL3 immediate direct targets

To determine whether the modest effects on the expression of tested trichome genes was a consequence of the low expression levels of the native GL3::GL3-GR transgene, and thus only a few cells being competent to enter the trichome pathway, I carried out similar experiments using *gl3 egl3/*p35S::GL3-GR plants. As was previously determined for p35S::R-GR plants (Lloyd *et al*., 1994), trichome initiation can be detected 24 hrs hours after DEX induction (see arrows, Fig. 2.2). Indeed, in *gl3 egl3*/p35S::GL3-GR plants, many trichomes form simultaneously without strictly following the ordered apical/basal pattern associated with developing leaves (Szymanski *et al*., 2000) and more trichomes were observed than in the corresponding *gl3 egl3*/pGL3::GL3-GR plants (not shown).

In contrast to what I established for *gl3 egl3*/pGL3::GL3-GR plants, GL2, CPC and ETC1 are robustly induced in *gl3 egl3/*p35S::GL3-GR plants within 4 hrs of DEX treatment, as shown by qRT-PCR (Fig 2.3A). Under these conditions, no induction of TRY was observed. To determine whether GL2, CPC and ETC1 are among the immediate GL3 targets, I exploited the post-translational regulation of GL3-GR by DEX, to distinguish between indirect downstream target genes (expression sensitive to the protein synthesis inhibitor cycloheximide, CHX) and immediate direct target genes (expression insensitive to CHX) (Sablowski and Meyerowitz, 1998). The induction by DEX of GL2, ETC1 and CPC, persisted even when the plants were treated with CHX and DEX (Fig. 2.3A), indicating these genes are most likely immediate direct targets of GL3.

To confirm the *in vivo* recruitment of GL3 to the promoters of *GL2*, *CPC* and *ETC1*, ChIP experiments were performed using antibodies against GR (αGR), in the presence and absence of 4 hrs of DEX treatment, in *gl3 egl3/*p35S::GL3-GR plants. ChIP results show a significant *in vivo* enrichment of GL3-GR at the promoter regions of all three genes in the presence of DEX, compared with Mock-treated plants (Fig. 2.3B), yet not to TRY, consistent with the expression results (Fig. 2.3A). In some cases, a low level of GL3-GR binding is observed in Mock-treated plants, suggesting perhaps a small amount of GL3-GR proteins enters the nucleus in the absence of the DEX ligand, although clearly not sufficient to complement the *gl3 egl3* mutant phenotype (Fig. 2.2). From these experiments, I conclude that GL3 directly activates *GL2*, *CPC* and *ETC1* expression at the early stages of trichome initiation.

GL3 auto-regulates its own expression

Models that attempt to explain trichome pattern formation often involve the self-activation of the regulators (Meinhardt and Gierer, 2000; Schellmann and Hulskamp, 2005). This prompted us to investigate whether *GL3* may regulate its own transcription. Thus, I explored the expression of *GL3* in *gl3 egl3/*pGL3::GL3-GR plants by qRT-PCR, in the presence and absence of DEX. After 4 hrs of induction with DEX, the accumulation of the GL3 mRNA was significantly decreased, compared to Mock-treated plants (Fig. 2.4A, pGL3::GL3-GR). Because the *gl3-1* allele present in the *gl3 egl3* plants is expressed at levels comparable to wild type (Payne *et al*., 2000), the level of *GL3* expression in this experiment corresponds to the sum of the endogenous *gl3-1* and the GL3-GR mRNAs. To further confirm the possibility that *GL3* might repress its own transcription, I investigated the expression of the *gl3-1* allele in *gl3 egl3/*p35S::GL3-GR plants, 4 hrs after DEX induction, using primers that distinguish between *gl3-1* and GL3-

GR. Again, DEX treatment resulted in a modest, yet significant, reduction in the steady-state levels of GL3 mRNA accumulation (Fig. 2.4A, p35S::GL3-GR). These results suggest the possibility of a negative feedback loop modulating *GL3* expression.

To determine whether GL3 is directly involved in this feedback regulation, expression analyses were repeated in the presence of 1) DEX and 2) DEX and CHX. As is often the case for immediate early genes in developmental processes (Edwards and Mahadevan, 1992), CHX significantly enhanced *GL3* mRNA accumulation, likely reflecting increased transcript stability (not shown). To correct for this, I normalized the qRT-PCR results to the levels of mRNA detected in plants treated just with CHX. The qRT-PCR experiments showed *GL3* mRNA reduction observed after DEX treatment in *gl3 eg3/*pGL3::GL3-GR plants remains in the presence of CHX (Fig. 2.4A). However, when similar CHX and DEX treatments were carried out in the *gl3 egl3*/p35S::GL3-GR plants, the expression of *GL3* was restored to the levels present in plants treated with CHX alone (Fig. 2.4A). Taken together, these results provide strong evidence for a model involving a negative auto-regulation of *GL3*. However, because CHX abolished GL3 self-repression in the *gl3 egl3*/p35S::GL3-GR plants, whether this involves direct interaction of GL3 with its own promoter still remains to be confirmed.

To unequivocally determine whether GL3 binds its own promoter *in vivo*, I performed ChIP experiments on *gl3 egl3/*p35S::GL3-GR plants, Mock-or DEX-treated for 4 hrs. A robust binding of GL3-GR to the *GL3* promoter (furnished by the *gl3-1* allele) is observed only in the presence of DEX (Fig. 2.4B), yet not in Mock-treated plants (Fig. 2.4B). I interpret these results to indicate that GL3 can bind to its own promoter, and that the overall result of this binding is a reduction in *GL3* expression.

GL1-Dependent and GL1-Independent GL3 Recruitment to DNA

The physical interaction of GL3 with GL1 (Zhang *et al*., 2003) was proposed to positively regulate trichome gene expression (Larkin *et al*., 2003; Marks and Esch, 2003; Schellmann and Hulskamp, 2005). I were therefore curious as to determine whether GL1 was required for the tethering of GL3 to the *GL3*, *CPC* and *GL2* promoters. Towards this goal, I expressed the previously described pGL3::GL3-YFP construct (Bernhardt *et al*., 2005) in *gl3 egl3* and *gl1* plants. I reasoned that, by using pGL3::GL3-YFP plants rather than DEX-induced pGL3::GL3-GR plants, I would be able to capture trichomes at all possible developmental stages, rather than at a single narrow developmental window furnished by the coordinate trichome formation provided by any given time after DEX treatment.

pGL3::GL3-YFP complements the *gl3 egl3* mutant phenotype, yet results in some trichome clusters (Fig. 2.5A). ChIP experiments were performed in both plants using antibodies against GFP (which cross-react with YFP). Interestingly, the *in vivo* recruitment of GL3-YFP to the *CPC* or *GL2* promoters is not observed in *gl1* mutants (Fig. 2.5B), supporting the model that the formation of a GL3/GL1 complex is necessary for the GL3 recruitment to these promoters. In contrast, GL3 binds its own promoter *in vivo* independently of GL1, since the binding is still present in *gl1* mutant plants (Fig. 2.5B).

While I could not observe GL3-GR recruitment to the TRY promoter in p35S::GL3-GR (Fig. 2.3) or pGL3::GL3-GR (not shown) plants induced with DEX for 4 hrs, GL3-YFP is clearly recruited to the promoter of this gene. Interestingly, however, the binding of GL3 to *TRY* is independent of *gl1* (Fig. 2.5B, TRY). The main difference between the GL3-GR and the GL3-YFP experiments is that in the former I assayed DNA-binding 4 hrs after the induction of trichome initiation, whereas in the latter, experiments

were performed using plants with trichomes at all possible developmental stages (Fig. 2.5A). Thus, GL3 binding to the *TRY* promoter might be associated with later aspects of GL3 function. Expression analyses by qRT-PCR support the GL1-dependent and GL1-independent GL3 regulatory activity described above, as the activation of transcription of *CPC*, *ETC1* and *GL2* except *TRY* in p35S::GL3-GR plants requires the presence of a functional *GL1* allele (Fig. 2.5C). While GL3-GR does not induce *TRY*, *TRY* expression is significantly reduced in *gl3 egl3* plants, compared to wild type plants (not shown). Taken together, these results indicate GL3 functions by both GL1-dependent and GL1-independent mechanisms.

DISCUSSION

Arabidopsis trichomes provide a powerful system to study plant epidermal cell differentiation and the bHLH transcription factors GL3/EGL3 play central functions in this process. Previous studies implicated *GL1* and *TTG1* in *GL2* regulation in the trichome developmental pathway (Szymanski *et al*., 1998). Our results show GL3 binds *in vivo* to and activates *GL2* transcription within 4 hrs of induction. Because this induction is observed even in the absence of *de novo* protein synthesis (Fig. 2.3A), I conclude that *GL2* is an immediate early direct target of GL3. In agreement with previous findings, this activity of GL3 is dependent on the presence of functional *GL1* (Fig. 2.5), supporting the model of a GL3-GL1-TTG1 complex responsible for *GL2* activation and subsequent trichome initiation.

In addition to putative GL1 binding sites (Szymanski *et al*., 1998), the *GL2* promoter contains multiple E-boxes, *cis*-regulatory elements likely responsible for the binding of GL3 or related bHLH factors. The recruitment of GL3 to the *GL2* promoter happens in the absence of *EGL3*, suggesting that the physical interaction between GL3

and EGL3 (Zhang *et al*., 2003) is not required for the GL3 DNA-binding activity. Indeed, the region involved in GL3-EGL3 interaction is likely to be the same region that mediates GL3 homodimerization (Zhang *et al*., 2003), located at the very end of the protein, C-terminal to the bHLH. This region is conserved among the R-like sub-group of bHLH factors (Feller *et al*., 2006). Our results provide the first direct *in vivo* evidence that R/GL3-like transcription factors can be recruited to the promoters of genes they regulate.

GL3 also binds to and controls the activation of *CPC* and *ETC1* early during trichome initiation in a fashion that is dependent on GL1 (Fig. 2.3 and 2.5). In agreement with epistasis analyses suggesting these proteins function upstream of GL2, our results show they are also immediate direct targets of GL3 (Fig. 2.3). *CPC* and *ETC1* encode single MYB-repeat proteins proposed to compete with GL1 for the interaction with GL3/EGL3, and accordingly, both GL3 and EGL3 physically interact with CPC (Zhang *et al*., 2003). Similar to *GL2*, *ETC1* and *CPC* promoters contain multiple candidate GL3- and GL1-binding sites. Indeed, previous studies demonstrated direct binding of WER to the *CPC* promoter (Koshino-Kimura *et al*., 2005).

However, our studies failed to detect either *TRY* activation or binding of GL3 to *TRY* soon (within 4 hrs) following GL3 induction (Fig. 2.3). Nevertheless, our results indicate that *TRY* is regulated by GL3, as evidenced by the significantly reduced *TRY* mRNA levels in *gl3 egl3*, compared to wild type plants (not shown), and by the *in vivo* recruitment of GL3-YFP to the *TRY* promoter in *gl3 egl3* plants harboring the pGL3::GL3-YFP construct, which display trichomes at various developmental stages (Fig. 2.5). The finding that GL3-YFP binds the TRY promoter is significant, as it demonstrates the inability of GL3-GR to bind to the TRY promoter is unlikely a consequence of probing for an incorrect promoter fragment in our ChIP experiments. Our results, suggesting a different regulation of TRY and CPC, complement functional

studies that propose similar, yet distinct activities for these two small MYB proteins in trichome patterning (Schellmann *et al*., 2002). While *TRY* mutants accumulate frequent trichome clusters, *CPC* mutants display no clusters, but ~2-fold increased trichome numbers. In addition, *TRY* mutants, but not *CPC,* display increased DNA content as a consequence of additional rounds of endoreduplication. Finally, the targets of CPC and TRY are likely to be different, based on the ability of p35S::GL1 or p35S::R to rescue only the trichome phenotype of p35S::TRY or p35S::CPC plants, respectively (Schnittger *et al*., 1999; Schellmann *et al*., 2002). Our results, indicating a delayed activation of *TRY* by GL3, are consistent with a later function of *TRY*, preventing in mature leaves the differentiation of accessory cells into trichomes (Schnittger *et al*., 1999).

I also found GL3 may participate in an auto-regulatory loop directly targeting its own promoter for transcriptional repression (Fig. 2.4). In contrast to the activation of *GL2*, *CPC* and *ETC1*, the recruitment of GL3 to its own promoter is independent of GL1, suggesting at least two distinct mechanisms by which GL3 can regulate gene expression. At first glance, the presence of a GL3 negative auto-regulatory loop appears to be in conflict with a model attempting to explain how, from a field of initially equivalent epidermal cells, trichome initials are selected (Meinhardt and Gierer, 1974, 2000). According to this model, the activators (GL3/GL1) stimulate their own expression and that of the negative regulators (*e.g.,* CPC, ETC1). The ability of the repressors to diffuse to adjacent cells, activity that has been shown for CPC in roots (Wada *et al*., 2002), together with the self-activation of the positive regulators would result in small differences in the concentration of the active complexes, and resulting in specific cells being selected for the trichome pathway. However, two possible explanations may reconcile such a model with our own results. It is possible that another trichome regulator working either upstream of GL3 or with GL3 (*e.g.,* GL1 or TTG1) is self-activated and

the observed GL3 auto-repression occurs temporally later, once the selection of trichome initials has occurred. An alternative explanation is the negative auto-regulation of GL3 I observed occurs in cells destined not to become trichomes, which are known to express reduced levels of *GL3* (Zhang *et al*., 2003). Perhaps, a negative auto-regulation of GL3 in non-trichome cells confounds a positive GL3 auto-regulation in trichome initials, just by the sheer larger number of the former. Experiments are currently under way to establish whether both positive and negative auto-regulatory loops govern GL3 expression in trichome and non-trichome cells, respectively.

In conclusion, our results provide evidence that the GL3 bHLH factor controls early events in the differentiation of epidermal cells into leaf hairs by directly binding the promoters of a set of genes, that when mutated, affect trichome patterning. Among these genes, only GL2 is a positive regulator of trichome initiation, while CPC, TRY and ETC1 are more likely involved in establishing leaf trichome patterns. It will be important to identify additional GL3 direct targets to determine whether the activation of GL2 by these bHLH factors is sufficient to trigger initiation into this developmental pathway.

Figure 2.1: Induction of trichome formation by *gl3 egl3*/pGL3::GL3-GR.

GL3-induced trichome formation in *gl3 egl3* /pGL3::GL3-GR seedlings treated with DEX. **A**, Mock-treated. **B**, treated with DEX.

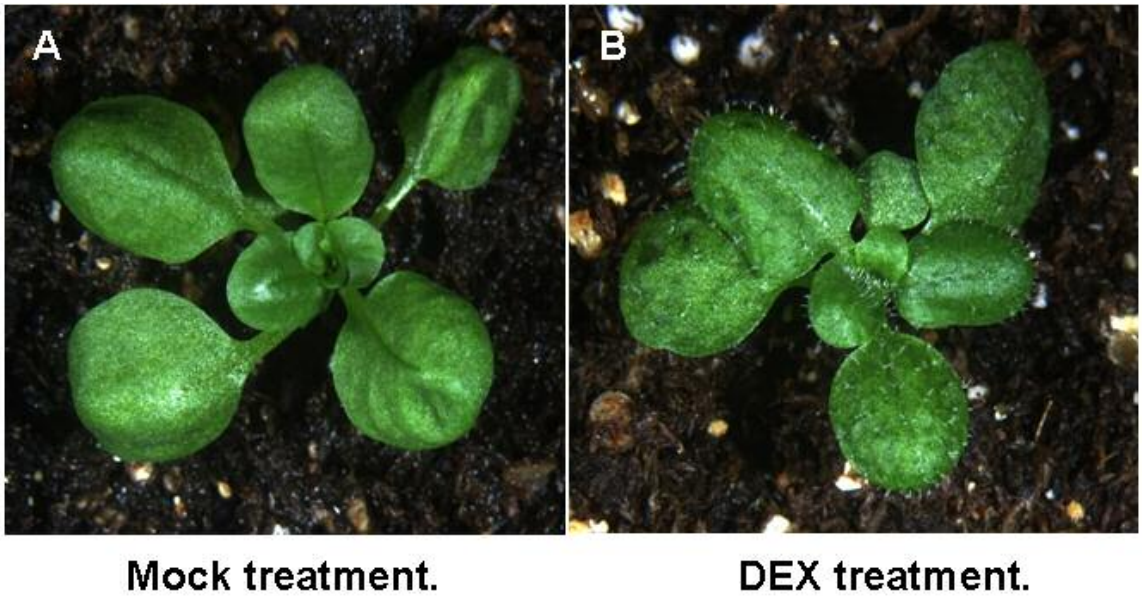

Figure 2.2: Coordinated trichome initiation by DEX treatment of *gl3 egl3*/p35S::GL3-GR seedlings.

SEM of *gl3 egl3/* p35S::GL3-GR seedlings 0, 12, 24, 36, 60 and 72 hours after induction with DEX. Arrows in 24 hrs indicate trichome initials. Scale bar = 20μm.

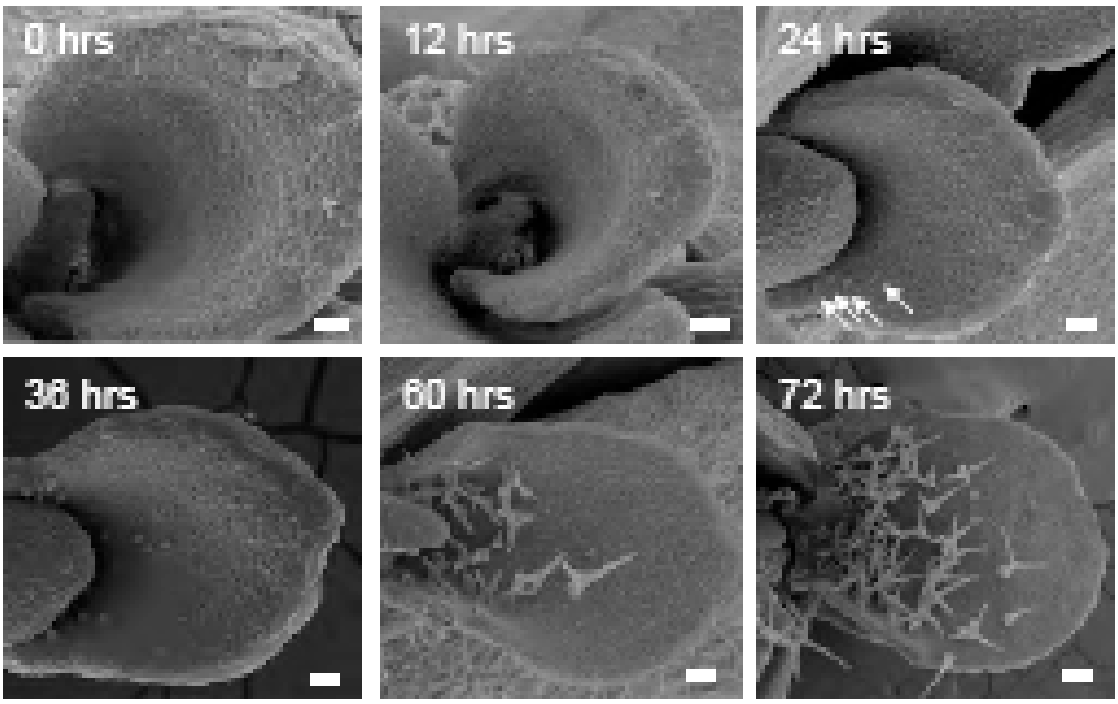

Figure 2.3: Identification of GL2, CPC and ETC1 as GL3 immediate direct targets.

A, qRT-PCR of mRNA obtained from green tissues of 10-days old *gl3 egl3* plants expressing p35S::GL3-GR treated with DEX (black), or DEX and CHX (hatched) for 4 hrs. The bars indicate the relative expression to Mock- or CHX treated plants, respectively. Relative expression was determined in triplicate measurements, and error bars indicate the standard deviation of the data. **B,** Semi-quantitative PCR of ChIP experiments of *egl3 gl3* p35S::GL3-GR plants Mock-treated (M) or treated with DEX (D) for 4 hrs. Input corresponds to the chromatin prior to immunoprecipitation, αGR to the material recovered after immunoprecipitation with antibodies against GR. PCR was performed on three four-fold serial dilutions of the ChIP-ed material, represented by the black slope on the top. The graph on the left indicates the position of the PCR fragment relative to the transcription start site (indicated by an arrow) of the various genes. At3g33520 and ACT2/7 correspond to negative controls.

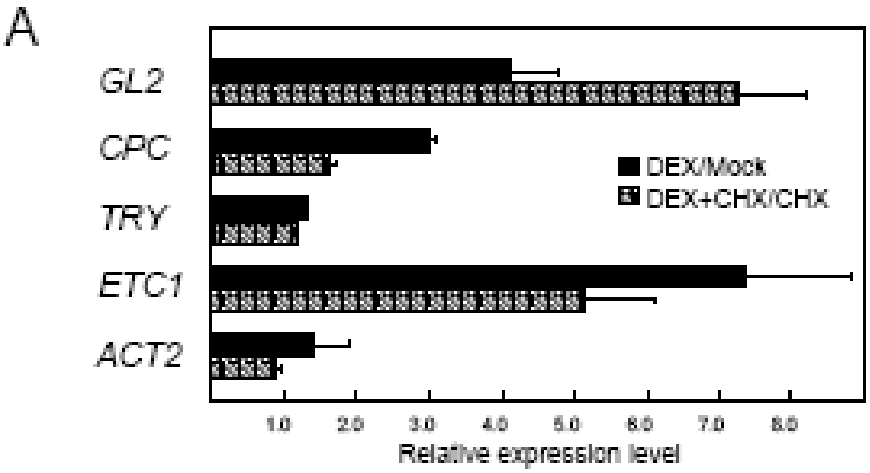
A
GL2
CPC
TRY
ETC1
ACT2
DEX/Mock
DEX+CHX/CHX
1.0
2.0
3.0
4.0
5.0
6.0
7.0
8.0
Relative expression level

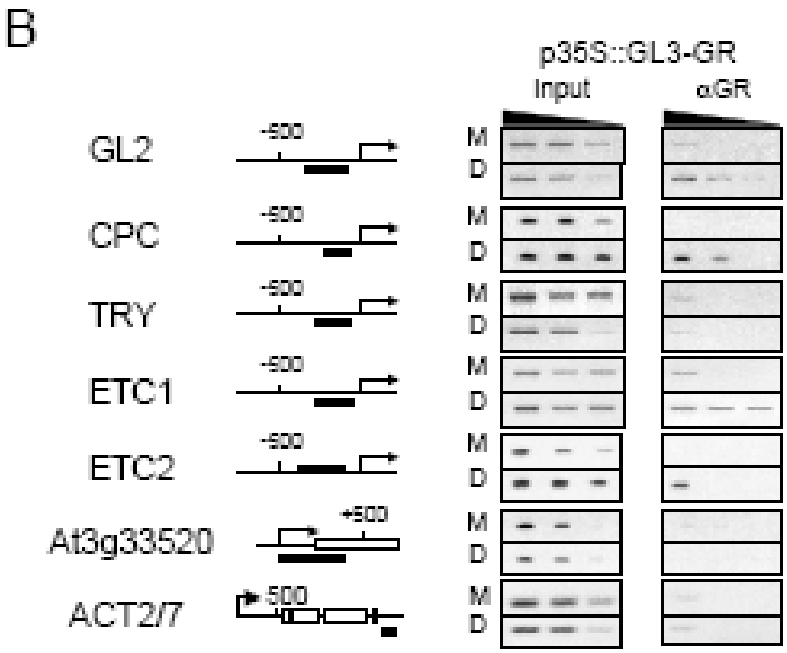
B
p35S::GL3-GR
Input
αGR
GL2
CPC
TRY
ETC1
ETC2
At3g33520
ACT2/7
-500
+500
M
D

Figure 2.4: *GL3* expression is controlled by an auto-feedback regulatory loop.

A, qRT-PCR of mRNA obtained from green tissues of 21-day old gl3 egl3 pGL3::GL3-GR (pGL3::GL3-GR) or gl3 egl3 p35S::GL3-GR (p35S::GL3-GR) treated for 4 hrs with DEX (black), or with DEX and CHX (hatched). The bars indicate the relative expression to Mock- or CHX treated plants, respectively. Relative expression was determined in triplicate measurements, and error bars indicate the standard deviations. For pGL3::GL3-GR, primers were designed to recognize both the endogenous GL3 transcript (from the gl3-1 allele) and the GL3-GR mRNA. For p35S::GL3-GR, primers recognized specifically the endogenous GL3 mRNA (from gl3-1). B, Semi-quantitative PCR of ChIP experiments carried out with chromatin obtained from green tissues of 20 day-old gl3 egl3 p35::GL3-GR plants Mock-treated (M) or treated with DEX (D) for 4 hrs. Input corresponds to the chromatin prior to immunoprecipitation, αGR to the material recovered after immunoprecipitation with antibodies against GR. PCRs were performed on three four-fold serial dilutions of the ChIP-ed material, represented by the black slope on the top. The graph on the left indicates the position of the PCR fragment relative to the transcription start site (indicated by an arrow) of the GL3 gene.

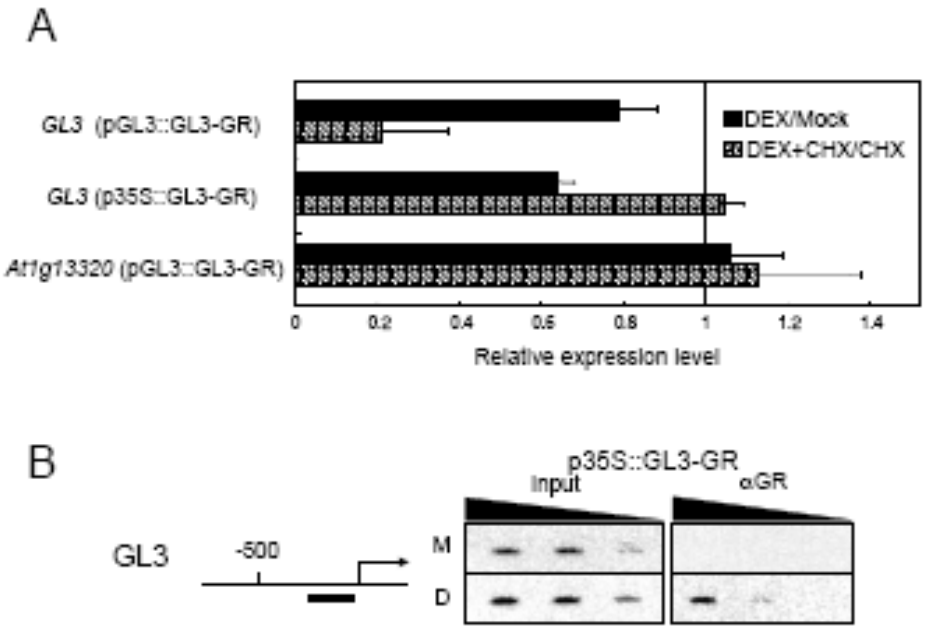

Figure 2.5: GL1-dependent and GL1-independent recruitment of GL3 to target promoters.

A, Complementation of the trichome phenotype of *gl3 egl3* mutants by pGL3::GL3-YFP (left), but not of *gl1* (center), which remain glabrous, compared to the wild-type *Ler* (right). Scale bar = 1 mm. **B,** Semi-quantitative PCR of ChIP experiments carried out with chromatin obtained from green tissues of 20 days-old *gl3 egl3*/pGL3::GL3-YFP (left), or *gl1/*pGL3::GL3-YFP (right) plants. PCRs were performed on three four-fold serial dilutions of the ChIP-ed material, represented by the black slope on the top. **C,** qRT-PCR of mRNA obtained from green tissues of 21-day old *gl3 egl3/* p35S::GL3-GR (black) or *gl1/*p35S::GL3-GR (diagonal) treated for 4 hrs with DEX (black), or with DEX and CHX (hatched). The bars indicate the relative expression to Mock-treated plants. Relative expression was determined in triplicate measurements, and error bars indicate the standard deviations.

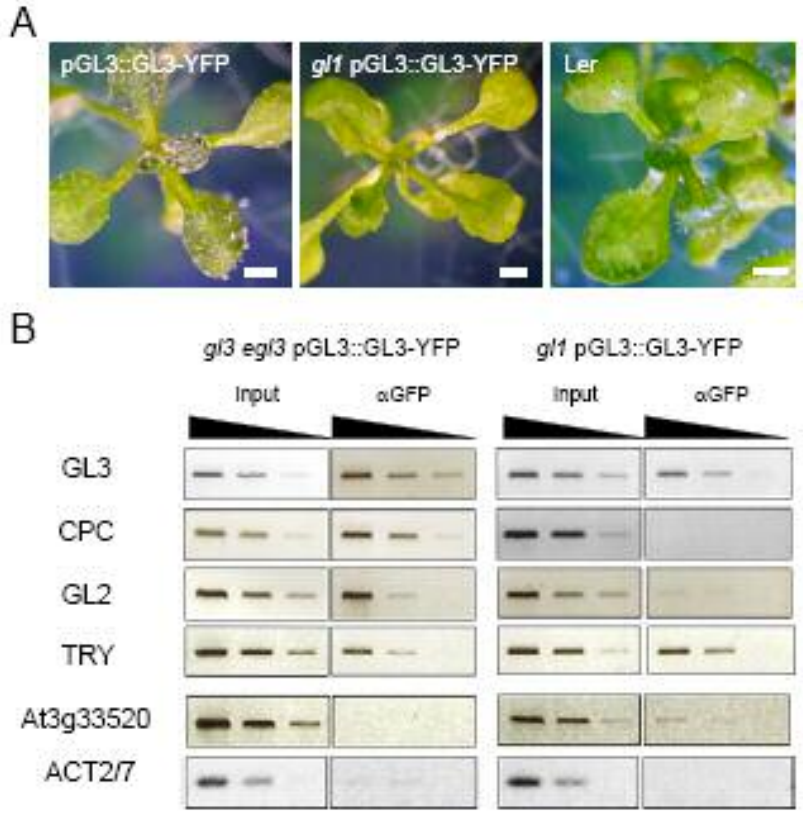

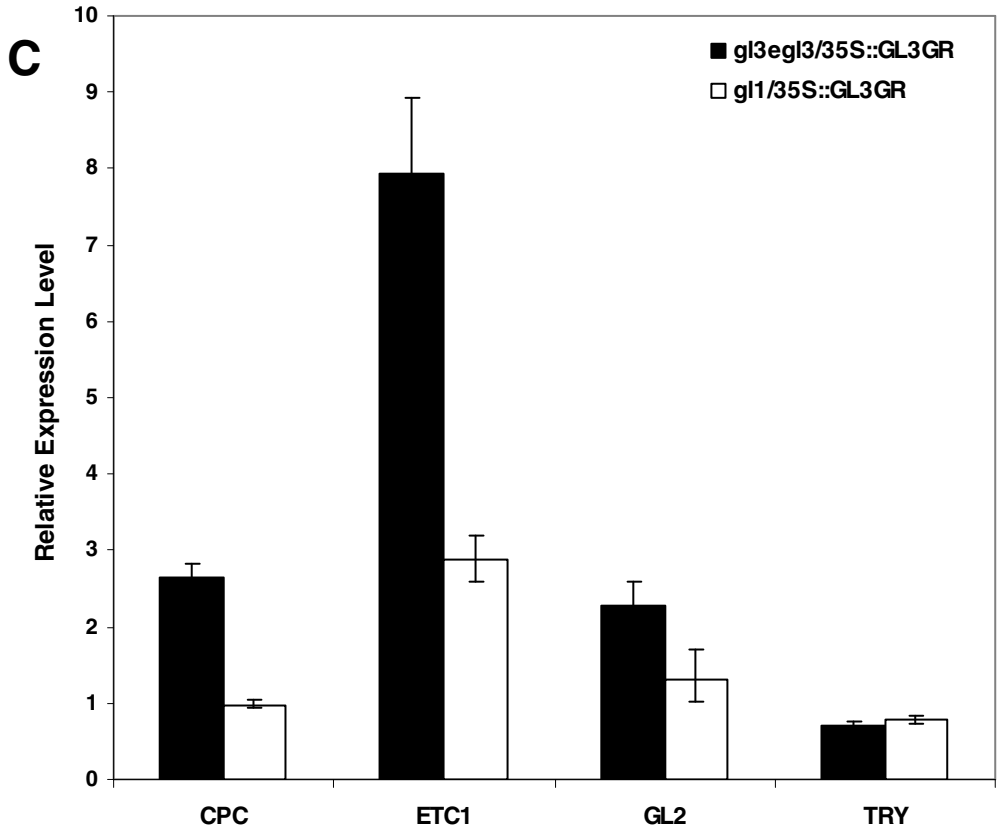
C
gl3egl3/35S::GL3GR
gl1/35S::GL3GR
Relative Expression Level
0
1
2
3
4
5
6
7
8
9
10
CPC
ETC1
GL2
TRY

Chapter 3: TTG1-bHLH-MYB complex regulates trichome initiation and patterning through direct targeting of trichome regulatory loci.

INTRODUCTION

Previous yeast two-hybrid assays have shown that TTG1 physically interacts with bHLH proteins, but not with itself, or with MYB transcription factors, such as GL1. Also from yeast two-hybrid experiments, it is known that the bHLH proteins, GL3 and EGL3, interact with GL1 (Payne *et al*. 2000; Zhang *et al*. 2003). Based on these data, it is proposed that TTG1 would form a TTG1-bHLH-MYB complex to regulate other trichome regulators.

In recent work, I have shown that GL3, GL2, CPC and ETC1 are direct targets of GL3 and this targeting is GL1 dependent (Chapter 2). The work presented here is aimed at further testing and refining details of the trichome development model under the control of the TTG1-bHLH-MYB complex. Here I show that the activators (GL2/TTG2) and repressors (CPC/ETC1) are major transcriptional targets for the complex. In addition, I also demonstrate the existence of the TTG1-bHLH-MYB complex in plants and show that loss of complex members disrupts the distribution of other complex members. Furthermore, I show that the repressor CPC moves in the leaf epidermis while none of the activators tested move. These results support and also add novel perspectives to the current model for trichome patterning.

MATERIAL AND METHODS

Plasmid constructions

All PCR amplification products used in construction were completely sequenced.

pTTG1::YFP-TTG1 and pTTG1::TTG1-cMYC: p5T3-5 was constructed by cloning a *TTG1* genomic fragment, which includes *TTG1* coding region with 5' and 3' regulatory sequences, into the pBluescript Plus vector. New *NotI* and *XbaI* restriction sites were generated by inverse PCR at the 5' end of the *TTG1* coding region using p5T3-5 as template. The *YFP*-coding region was amplified from pEYFP (Clontech) and ligated in-frame to the *TTG1 5'* end using ***Not***I and ***Xba***I sites to make pYFP-TTG1. To create the fusion gene TTG1-cMYC, p5T3-5 was modified by inverse PCR so that the stop codon of *TTG1* was removed and replaced by new *Not*I and *Xba*I restriction sites. The result vector was named pTINV. A fragment containing 5 copies of the cMYC epitope was amplified from pCS2+MT (Roth ***et al***. 1991) and ligated in-frame into ***Not***I and ***Xba***I sites of pTINV to make pTTG1-cMYC. Fragments digested from pYFP-TTG1 and pTTG1-cMYC by *EcoR*I and ***Sac***I, containing entire TTG1::*YFP-TTG1 and TTG1::TTG1-cMYC* fusions, were subcloned into the same sites of the T-DNA vector pAL47 (Lloyd and Davis, 1994) to create pTTG1::YFP-TTG1 and pTTG1::TTG1-cMYC.

pGL1::GL1-YFP-cMYC and pGL1::GL1-YFP-6His: A 3kb fragment, containing GL1 5' promoter and coding region without stop codon, was amplified from *Ler* genomic DNA and cloned into the pBluescript Plus vector using *KpnI* and *HindIII* restriction sites to create pBGL1.

To add cMYC epitope tags between *GL1* coding region and its 3' downstream regulatory region, I used a "combinatory PCR" technique. The first fragment was amplified using pCS2+MT (Roth ***et al***. 1991) as template so that a 13-nucleitide-long sequence of the 5'end of the ***GL1*** 3' downstream region was added after the stop codon of 5XcMYC. Then the second fragment was amplified from genomic DNA, which contained about 1kb GL1 3' downstream region starting with a 15-nucleitide-long

sequence of the 3' end of the 5XcMYC sequence. These two fragments were re-annealed and used as the template for the third round of PCR to amplify the fusion 5XcMYC-GL1 downstream, which was then digested and inserted into ***Hind***III and ***BamH***I sites of the pBluescript Plus vector to make pMter. Confirmed by sequencing, pBGL1 and pMter were digested by *Hind*III and *BamH*I and ligated to make pGL1::GL1-MYC, which was modified by inverse PCR so that a new *Xba*I restriction site was generated between the *Hind*III site and the start codon of 5XcMYC. A *Kpn*I-*BamH*I fragment from this vector, which contained the entire GL1::GL1-MYC fusion, was subcloned into the same sites of pAL47 to create pGL1::GL1-MYC-INV. The *YFP*-coding region without the stop codon and a YFP-6XHis fusion were amplified from pEYFP and ligated into ***Hind***III and ***Xba***I sites of pGL1::GL1-MYC-INV to make pGL1::GL1-YFP-cMYC and pGL1::GL1-YFP-6His respectively.

p35S::HA-GL3-6His: A fragment containing the GL3 coding region with HA fused to 5' end and 6XHis epitope tag inserted before the stop codon, plus Gateway recombination sequences on both ends was amplified from genomic DNA and recombined into the Gateway site of the vector pDonor222 (Invitrogen) to create pGWHA-GL3-6His. pGWHA-GL3-6His was recombined with pB7WG2 (Karimi ***et al.***, 2002) to make p35S::HA-GL3-6His containing HA-GL3-6His under *CaMV35S* control.

P35S::GL3-GR was described in chapter 2.

p35S::GL3-YFP, p35S::GL1-YFP, p35S::GL2-YFP and ***p35S::YFP-CPC***: Fragments containing the entire genomic coding region of GL3/GL1 with stop codon removed or GL2 cDNA minus stop codon or the entire CPC cDNA, plus Gateway recombination sequences on both ends, were amplified and recombined into the Gateway site of the vector pDonor222 (Invitrogen) to create pGWGL3, pGWGL1, pGWGL2 and pGWCPC respectively. pGWGL3 and pGWGL1 were recombined with pB7CWG2

(Karimi ***et al.***, 2002) to make p35S::GL3-YFP and p35S::GL1-YFP. pGWGL2 was recombined with pK7YWG2 (Karimi ***et al.*** 2002) and pGWCPC was recombined with pZYWG7 (Karimi ***et al.*** 2002) to make p35S::GL2-YFP and p35S::YFP-CPC.

pEGL3::GUS contains 3 kb of DNA upstream of the *EGL3* coding region inserted in front of the *GUS* gene in pBG1.1 (Gray-Mitsumune *et al*. 1999).

Plant materials and growth conditions

The following transgenic lines have been described previously:

*Ler/*pGL3::GUS was described as in *gl3 egl3/*p35S::GL3-GR was described as in Chapter 2. The seeds from transgenic plants *ttg1*/p35S::TTG1-GR (Baudry *et al*. 2006) were generously provided by Dr. Loic Lepiniec. *Ler/*pGL3::GUS (Zhang *et al*., 2003) and *gl3-2*/pGL3::GL3-YFP (Bernhardt *et al*., 2005) were described in publication. *gl3-2*/pGL3::GL3-YFP was crossed to *gl1* and *gl1*/pGL1::GL1-YFP-cMYC was crossed to *ttg1* to make *gl1*/pGL3::GL3-YFP and *ttg1*/pGL1::GL1-YFP-cMYC respectively, which were confirmed by YFP fluorescence microscopy. Transgenic lines expressing both pTTG1::TTG1-cMYC and pGL1::GL1-YFP-6His fusions was created by crossing *gl1*/pGL1::GL1-YFP-6His to *ttg1*/ pTTG1::TTG1-cMYC. Appropriate F2 plants were confirmed by YFP fluorescence microscopy and western blots probed against cMYC. Transgenic lines expressing both pTTG1::TTG1-cMYC and p35S::HA-GL3-6His fusions was created by transforming *ttg1*/ pTTG1::TTG1-cMYC plants with p35S::HA-GL3-6His. Transformants were identified by kanamycin and BASTA resistance. Other transgenic plants were created by floral dip transformation, unless otherwise indicated. Standard plant crosses were done with two homozygotes and the F1 was selfed to identify proper progeny.

Arabidopsis thaliana plants were grown on soil at 21^{o}C in continuous white light.

Gene expression analyses

Seedlings were grown on germination media containing 3% sucrose at 21° C in continuous white light. Four-day-old seedlings were treated with 20 uM dexamethasome or mock-treated with 0.001% ethanol for four hours, then washed with water and frozen in liquid nitrogen. For the cyclohexamide treatment, I used 100 uM CHX. Total RNA was prepared using the Qiagen plant RNeasy mini kit. 4 ug RNA was used in 20 ul reverse transcription reactions containing 250 nM Actin and target gene specific reverse primers. Parallel PCR reactions using reverse transcription reactions as template were set up in a total volume of 25 ul with 12.5 ul 2X SuperPower Syber mixture (ABI) and run on a spectrofluorometric thermal cycler (ABI 7900HT). For each target five PCR reactions containing 400 nM primer and 3 ul first strand cDNA template were performed along side four actin control PCR reactions containing 200 nM Actin primers and 1 ul first strand actin cDNA. The PCR cycling parameters used were as follows: 95° C, 10 min, 40 cycles of 95° C, 15 sec and 60° C, 1 min. The comparative cycle threshold method was used to analyze the results of Q-PCR (User Bulletin 2, ABI PRISM Sequence Detection System). This experiment was performed twice for each target with consistent results. Results of a representative experiment are presented.

Chromatin Immunoprecipitation (ChIP) Experiments

ChIP experiments were performed as described in Chapter 2.

Microscopy

Plant tissues were mounted in water for microscopy. The histochemical analysis of plants containing the *GUS* reporter constructs was performed with at least 5 seedlings for each strain essentially as described (Masucci *et al*., 1996).

Imaging of YFP fusions was performed on Leica SP2 AOBS confocal laser scanning microscope with excitation (514 nm) and emissions (530–600 nm for YFP and 675-800 for chlorophyll). Collected images were processed for maxium intensity projection and fluorescence quantification using MetaMorph Version 6.1r6 software (Universal Imaging Corp). For calculating cytoplasmic and total fluorescent intensities, sum of the total signal above the background threshold was calculated as the total fluorescent intensity. The sum of the signal between the background threshold and the nuclear threshold was caculated as the cytoplasmic fluorescent intensity.

Microprojectile Bombardment

Tangsten particles (1.5 mg) were coated with approximately 5 mg of each plasmid DNA as directed by the manufacturer's instructions (Bio-Rad). Young leaves from *gl3 egl3* double mutant plants were excised, placed onto MS plates and bombarded at a pressure of 1100 psi with flight distance of 15 cm by using a helium biolistic device (Bio-Rad PDS-1000). Bombarded leaves were grown overnight under white light, examined for YFP fluorescence at low magnification by using a fluorescence dissecting microscope (Nikon) and then imaged on the confocal microscope at higher magnification. More than five independent bombardment events have been examined.

Co-precipitation experiments

Three-week-old *Arabidopsis* green tissue was collected and ground into fine powder in liquid nitrogen. Protein extract was prepared by mixing 0.1 g powder well with 1 ml ice-cold buffer A (50 mM Tris, 100 mM NaCl, 10 mM MgCl2, 10% glycerol, 1 mM DTT, 1% Triton-X100, 1 mM PMSF, 1 ug/ml (Leupeptin, Antipain, Pepstatin A, Aprotinin) each, 5 mM Imidazole, pH 7.3) in a 1.5 ml eppendorf tube. The mixture was centrifuged twice at 13000 rpm for 10 min, and the supernatant was used as input extract. 0.9 ml of the input extract was applied to a pre-equilibrated His-select column (with buffer A), washed (with buffer A containing 45 mM imidazole) and eluted (with buffer A containing 300 mM imidazole) as directed by the manufacturer's instructions (Sigma). The elution was concentrated with Microcon Y-M30 filter (Millipore). Input extracts and concentrated eluates were mixed with loading buffer to final volume of 100 ul and boiled for 5 min prior to loading the SDS-PAGE gel (Bio-Rad). 2 ul of input and 5 ul of elution loading samples were used for western blots which were probed by anti-cMYC monoclonal antibody 9E10 (Santa Cruz biotechnology) and visualized by Western Lightning Chemiluminescence Reagents (Amersham Biosciences).

RESULTS

TTG1 is expressed ubiquitously on *Arabidopsis* leaves

The transcription of *TTG1* is detected in all major organs of *Arabidopsis* (Walker *et al*. 1999). To study the expression of TTG1 protein during the process of trichome initiation and patterning, I examined YFP fluorescence of a TTG1::YFP fusion protein under the control of the native TTG1 promoter in the *ttg1* mutant background *(ttg1*/pTTG1::YFP-TTG1). The transgenic *ttg1*/pTTG1::YFP-TTG1 plants showed wild type trichome formation (Fig. 3.1), as well as normal anthocyanin production and seed coat pigment and differentiation (not shown), indicating that the translational TTG1-YFP fusion was functional. Figure 3.1A shows that the TTG1 protein is present in all epidermal cells and trichomes at all developmental stages. This ubiquitous and persistent expression pattern was further confirmed by a close-up view of the YFP expression in stage-4 trichomes (Szymanski *et al*. 1998) and their surrounding epidermal cells (Fig. 3.1B). At earlier stages I see strong YFP signal in the nuclei of trichome initials and all pavement cells as well as a much weaker YFP signal in the cytoplasm of these same cells (Fig. 3.1C). TTG1 protein appears to be expressed at all stages of leaf and trichome development. Quantification of the fluorescence distribution indicates that a significant amount of TTG1 localizes to the cytoplasm although the majority of TTG1 appears to be nuclear (Fig. 3.4E)

TTG1 regulates GL3 target genes

GL3 has been reported to directly target trichome development genes, both trichome initiation activators and repressors. To better define the trichome genes regulated by the TTG1-bHLH-MYB regulatory complex, the expression changes of

previously identified GL3 targets including *GL3, GL2, ETC1* and *CPC* (Fig. 2.3A) were investigated by QPCR in DEX-treated *ttg1*/p35S::TTG1-GR plants, in the presence or absence of cycloheximide (CHX). The TTG1-GR fusion complements *ttg1* mutants only with the addition of DEX. Simultaneous treatment with DEX and CHX blocks de novo protein production and allows only the direct targets to be transcribed (Sablowski and Meyerowitz 1998). This same TTG1-GR fusion has been used to show that the bHLH, TT8, was directly activated by TTG1 in *A. thaliana* siliques (Baudry *et al*. 2004). In other work, I have shown that this fusion provides DEX dependent activation of the late anthocyanin structural genes (Fig. 4.3).

As shown in Fig. 3.2A, GL2, CPC and ETC1 were up-regulated in response to the 4-hours induction by DEX, while the expression of GL3, TRY and ETC2 did not change. This experiment was repeated with a DEX plus CHX treatment. I found that GL2, CPC, and ETC1 again were up-regulated, but to a lower level (Fig. 3.2A). To confirm these expression results, I conducted chromatin immunoprecipitation (ChIP) experiments with *ttg1*/pTTG1::YFP-TTG1 plants, using antibodies against GFP which cross-react with YFP. Similar to what I previously described for GL3 (Fig. 2.3B), YFP-TTG1 was recruited to the promoters of GL2 and CPC *in vivo* (Fig. 3.2B). However, YFP-TTG1 was not found to bind to the promoter of ETC1, possibly for unknown technical reasons. I also acknowledge the possibility that ETC1 is TTG1-independent. These results show that GL2, CPC and perhaps ETC1 are immediate direct targets of TTG1, indicating that TTG1 and GL3 share many of the same targets.

TTG2 is an immediate direct target of TTG1 and GL3

TRANSPARENT TESTA GLABRA2 (TTG2) is a trichome development gene of *Arabidopsis*, encoding a WRKY transcription factor. Genetic data suggests that TTG2

functions downstream of TTG1 and GL1 and its expression requires TTG1 function in leaf primordia (Johnson *et al*. 2002), suggesting that TTG1 and GL1 may directly control TTG2 expression in the leaf tissue. By similar approaches, I analyzed 35S::TTG1-GR transgenic seedlings and 35S::GL3-GR transgenic *gl3 egl3* seedlings for expression changes in TTG2 after DEX induction. Four hour DEX induction of TTG1-GR and GL3-GR resulted in the up-regulation of TTG2 (Fig. 3.2A). Inclusion of DEX and CHX also resulted in the induction of TTG2 and identifies it as a direct target of both TTG1 and GL3, which is further supported by the ChIP result showing that TTG1 binds to the promoter of TTG2 *in vivo* (Fig. 3.2B).

It was previously shown that the R2R3-MYB, Werewolf (WER), binds the CPC promoter *in vitro* (Koshino-Kimura *et al*. 2005; Ryu *et al*. 2005) and I have shown that GL3 binds the promoter of GL2, CPC, ETC1 and GL3 *in vivo.* The binding of GL3 to the CPC and GL2 promoters is dependent on the presence of GL1 while binding to its own promoter is not (Fig. 2.5B). I used *gl1*/ pGL1::GL1-YFP-cMYC plants to perform ChIP experiments to investigate the *in vivo* binding of GL1 to the promoters of these known GL3 targets. GL1 was found to bind to the promoters of CPC, ETC1 and GL2, as well as that of TTG2, but not of GL3 (Fig. 3.2B). These results suggest that GL1 participates with GL3 in the regulation of GL2, CPC, ETC1 and TTG2, but not in the regulation of GL3. Taken together with the findings that GL2, TTG2, CPC and possibly ETC1 are direct transcriptional targets of both GL3 and TTG1, while GL3 is only regulated by itself, I conclude that GL2, TTG2 and CPC are activated minimally by a complex containing TTG1, GL3 and GL1.

TTG1 interacts with GL3 and GL1 in vivo

The gene expression studies presented above support the hypothesis that TTG1 would form a TTG1-bHLH-MYB complex (Payne *et al*. 2000; Zhang *et al*. 2003) to regulate other trichome regulators. To study this complex *in vivo*, I performed co-precipitation assays to test whether TTG1 interacts with GL3. The pTTG1::TTG1-cMYC and p35S::HA-GL3-6His fusions are functional in promoting trichome differentiation in *ttg1* and *gl3 egl3* mutants respectively. As shown in Fig. 3.3A, I could detect the TTG1-cMYC fusion in the input protein extractions in plants containing this construct (lanes 1 and 3; there is an artifactual smudge in lane 2, minus the TTG1-cMYC fusion) using an anti-cMYC monoclonal antibody. However, when I used His-select Ni columns to pull down the HA-GL3-6His fusion protein from these extracts, I were only able to detect TTG1-cMYC in the line containing both fusion proteins (Fig. 3.3A lane 6). This result demonstrates that TTG1 interacts with GL3 *in vivo*.

Using the same approach, I also tested for the interaction between TTG1 and GL1 *in vivo*. Strikingly, TTG1-cMYC was pulled down by the His-select Ni columns only when it was co-expressed with GL1::GL1-YFP-6His (Fig. 3.3B lane 6), while TTG1-cMYC was not detected in the samples processed from *ttg1*/pTTG1::TTG1-cMYC or *gl1*/pGL1:: GL1-YFP-6His (Fig. 3.3B lanes 4, 5). This result demonstrates that TTG1 interacts with GL1 *in vivo*.

The GL3/EGL3 bHLH proteins modulate the nuclear localization of TTG1

Because TTG1 possesses no identifiable nuclear localization signal, it may form a TTG1-bHLH complex or a TTG1-bHLH-MYB complex in the cytoplasm first, and then be transported into the nucleus and/or the complex could be required to retain TTG1 in the nucleus. If so, bHLH proteins may be required for the nuclear localization of TTG1.

To test this hypothesis, I examined the subcellular localization of YFP-TTG1 in the *gl3 egl3* mutant background. I observed uniform nuclear distribution of TTG1::YFP-TTG1 in leaves of *gl3 egl3* plants. Interestingly, I also detected a significant higher (20% in Fig. 3.4E) level of YFP signal in the cytoplasm of these plants compared to plants wild type for GL3 and EGL3 (compare Fig. 3.4A to B). In contrast, almost the same level of GL1-YFP signal (Fig. 3.4E) was detected in the cytoplasm of *gl3 egl3* epidermal cells as in wild type cells (Fig. 3.4C and D). This suggests that mutations in bHLH proteins cause higher levels of cytoplasmic TTG1, indicating that bHLH proteins affect the nuclear localization of TTG1 but not of GL1.

Loss of TTG1 and GL1 disrupts the nuclear distribution of GL3

I then performed the reciprocal experiment to test whether TTG1 and GL1 affect the GL3 protein distribution pattern in the leaf epidermis. Functional fusions of pGL3::GL3-YFP and p35S::GL3-YFP were introduced into the *ttg1* mutant background. I found that loss of TTG1 did not cause obvious changes in GL3's partitioning to the nucleus (compare Fig. 3.5A with Fig. 3.7F). However, compared to a uniform YFP fluorescent pattern exhibited by *gl3-2*/pGL3::GL3-YFP (Fig. 3.7F), the GL3-YFP protein was unevenly distributed into speckles in the nuclei of epidermal cells of both the *ttg1*/ GL3::GL3-YFP and *ttg1*/p35S::GL3-YFP leaves (Fig 3.5A and B). When I expressed GL1::GL1-YFP-cMYC and 35S::GL1-YFP in *ttg1* mutants, almost all epidermal nuclei showed evenly distributed GL1-YFP with only a couple of speckles (Fig. 3.5C and D). These results suggest that TTG1 is required for the proper subnuclear distribution of GL3. Although it is difficult to quantitatively compare these images, it does not appear that loss of TTG1 affects the stability of the GL3-YFP fusion.

To test whether mutations in GL1 might affect the distribution of GL3, I examined the subcellular localization of GL3-YFP in *gl1* mutants. When GL3-YFP was expressed under its native promoter in the *gl1* mutant, I found that GL3 still partitioned to the nucleus. However, just like with the *ttg1* mutant, GL3 formed speckles in the nuclei of leaf epidermal cells (Fig. 3.5E). In the roots of the same transgenic plant, where WEREWOLF, a GL1 functional homolog functions, GL3::GL3-YFP showed wild type patterning with no speckles (Fig. 3.5G). When GL3-YFP was overexpressed in the *gl1* mutant, more nuclear speckles were detected (Fig. 3.5F) in the leaf epidermis while uniform YFP signal was still observed in cell layers and cell files in the roots (Fig. 3.5H). These results suggest that GL1 is specifically required for the normal distribution of GL3 within the nuclei of *Arabidopsis* leaf cells.

Taken together, our studies on *in vivo* protein interactions and the subcellular localization of fluorescence fusion proteins show that TTG1, bHLH and GL1 form a nuclear complex *in vivo*. Moreover, the loss of specific complex members leads to an abnormal speckled distribution of GL3, a key complex member, possibly due to aggregation.

CPC moves in leaf epidermal cells

It has been shown that GL3 and CPC traffic from cell to cell in *Arabidopsis* roots (Wada *et al*. 2002; Bernhardt *et al*. 2005). I asked whether they or other trichome regulatory proteins could also traffic in the leaf epidermis. I made constructs to overexpress GL3, GL1, GL2, and CPC, which are fused in frame with YFP. pTTG1::YFP-TTG1 was constructed to express YFP-TTG1 fusion. The DNA constructs were introduced into developing leaf tissue by micro-projectile bombardment and were scored after overnight expression. During these experiments, I also bombarded a GUS

construct and I did not detect any area with clusters of transformed GUS-expressing cells, indicating that the probability of bombarding adjacent cells is very low (data not shown).

I repetitively observed extensive trafficking of the CPC-YFP fusion into adjacent cells as evidenced by cytoplasmic and nuclear YFP signal, generating clusters of up to 15 fluorescent cells in the *Arabidopsis* leaf epidermis. In contrast, I did not observe the same fluorescent pattern with any of the other fusion proteins, which were expressed in isolated single cells (Fig. 3.6). These results show that CPC can move in the leaf epidermis, but that GL3 does not. Our results, showing that CPC but not GL3 moves in the leaf epidermis contrast with our previous findings that they both move in roots. This probably reflects that fact that trichome patterning and root hair patterning are not regulated by the same mechanisms, although they largely share the same hierarchy of regulatory genes.

GL3 and EGL3 have overlapping but distinct transcription patterns

Our previous studies showed that GL3 and EGL3 are partially redundant in regulating trichome initiation. Both single mutants initiate fewer trichomes than wild type while the double mutant is completely glabrous (Zhang *et al*. 2003). However, single *gl3* mutants show a much more severe reduction in trichome initiation and branching than *egl3*. I also showed that GL3 and EGL3 are expressed with roughly similar patterns in leaves and roots, however, I also noted that EGL3 always seemed to be expressed at higher levels than GL3 (Payne *et al*. 2000; Zhang *et al*. 2003; Bernhardt *et al*. 2005). In order to begin to analyze this expression/phenotype difference, I carefully examined the Promoter::GUS expression patterns of GL3 and EGL3 during trichome development.

In young developing leaves of *Ler*/pGL3::GUS plants, GUS activity is observed in trichomes and surrounding epidermal cells especially in the region close to the basal edge of the leaf, with trichomes often showing significantly higher levels of GUS

activity. In more mature areas of the leaf, strong pGL3::GUS activity persists only in trichomes (Fig. 3.7A and B). In *Ler*/pEGL3::GUS plants, the maximum GUS activity was observed in young leaf primodia. In developing leaves, high pEGL3::GUS activity is observed in the basal one third region of the leaf. Lower levels of pEGL3::GUS activity are also observed in trichomes and epidermal cells in older leaves (Fig. 3.7D). Compared to pGL3::GUS, pEGL3::GUS exhibits a more widely distributed expression pattern with higher GUS activity in the epidermal pavement cells and lower GUS activity in trichomes. High pEGL3::GUS activity is also observed in the petioles of leaves while pGL3::GUS is not. Taken together, GL3 and EGL3 show overlapping, yet distinct transcription patterns during trichome development.

GL3 protein disappears in the pavement cells while EGL3 protein does not

The pGL3::GL3-YFP and pEGL*3*::EGL3-YFP fusions were constructed and shown to be fully functional by rescuing *gl3* and *gl3 egl3* mutants respectively. The analysis of the YFP fluorescence profiles of representative p*GL3*::GL3-YFP and p*EGL3*::EGL3-YFP containing transgenic plants shows that the protein expression profiles of GL3 and EGL3 match well with their transcription patterns respectively.

In the basal region of the developing leaf, where trichomes continue to initiate, strong GL3-YFP signal was detected in the nuclei of unbranched trichome initials (Fig. 3.7F arrow), while only a very weak GL3-YFP signal was occasionally detected in the neighboring non-trichome cells. In the more mature regions distal from the plant, GL3-YFP signal was completely restricted to the branching and mature trichomes and disappeared from non-trichome cells (not shown). In a developing leaf, as a trichome matures, the level of GL3-YFP intensity keeps decreasing until it completely disappears (not shown). Like GL3-YFP, EGL3-YFP was also found in the nuclei of unbranched

trichome initials in the leaf basal region. However, strong EGL3-YFP was also detected in the non trichome cells throughout the epidermal layer of a developing leaf (Fig. 3.7G and H). In a fully developed leaf, I found that p*EGL3*::EGL3-YFP remained detectable far longer than p*GL3*::GL3-YFP (not shown).

However, a comparison of patterns of p*GL3*::GUS and p*GL3*::GL3-YFP reveals a difference between the transcription pattern and the protein expression pattern of GL3. Significant p*GL3*::GUS activity was observed in the epidermal cells that neighbor young trichomes where GL3 protein is absent (compare Fig. 3.7A and G). Taken together with the finding that EGL3 gene is expressed and the EGL3 protein accumulates in non-trichome cells, these data imply that EGL3 functions within the non-trichome cell in the maintenance of the non-trichome cell fate, while GL3 does not.

DISCUSSION

TTG1 forms a TTG1-bHLH complex for nuclear import?

The *Arabidopsis* TTG1 locus encodes a WD40 protein containing four or more WD40 repeat motifs (Walker *et al*. 1999). A common function of WD40 repeat motifs is to facilitate protein-protein interactions. A preponderance of indirect evidence indicated that TTG1 interacts with bHLH proteins (GL3, EGL3 and TT8) in regulating all TTG1-dependent development pathways. The evidence includes: (1) *gl3 egl3 tt8* triple mutant phenocopies *ttg1* mutants and, (2) TTG1 physically interacts with GL3, EGL3 and TT8 in the yeast-two hybrid system (Payne *et al*. 2000; Zhang *et al*. 2003; Baudry *et al*. 2004). Because the TTG1 sequence contains no recognizable nuclear localization signal or DNA binding motif or transcriptional activation domain, it seems probable that TTG1 does not directly act as a transcription factor. TTG1 may form a complex with bHLH proteins for nuclear import or retention and/or act as a transcriptional co-regulator. Prior to the present study, it was also possible that TTG1 was located only in the cytoplasm possibly as a signal transduction component to regulate bHLH proteins. A cytoplasmic location would be in agreement with the reported location of AN11 (de Vetten *et al*. 1997) (a petunia WD40 protein which is highly similar to TTG1 and complements the *ttg1* mutation (not shown)). In this paper, I report that TTG1 is preferentially localized in the nucleus in the *Arabidopsis* leaf epidermis (Fig. 3.1), with a lower, yet significant, amount of TTG1 in the cytoplasm. This result indicates that TTG1 could function both as a transcriptional co-regulator in the nucleus and as a protein-interacting factor in the cytoplasm. I also show that TTG1 interacts with GL3 *in vivo* and the loss of GL3 and EGL3 causes an increased level of TTG1 in the cytoplasm (Fig. 3.4). I conclude that

bHLH proteins facilitate the nuclear import or retention of TTG1 proteins. In *gl3 egl3* mutants, there are other functional TTG1 interacting bHLH proteins such as TT8 and ATMYC1, which could also be functioning to guide TTG1 to the nucleus or retain it there. It will be interesting to see if TTG1 is even more cytoplasmic in a bHLH quadruple mutant.

The TTG1-bHLH-MYB regulatory complex

Although I have demonstrated that TTG1 interacts with bHLH proteins *in vivo*, and that loss of bHLH proteins leads to increased cytoplasmic TTG1, the biological significance of the TTG1-bHLH interaction still remains to be elucidated. Our previous genetic data (Zhang *et al*. 2003), together with the results discussed in this paper, favors the possibility that TTG1 functions as a transcription co-regulator. TTG1 may modify, stabilize or in some other fashion positively affect GL3/EGL3 in their capacity to activate the transcription of downstream target genes. Our earlier work on the regulation of the anthocyanin pathway showed that GL3 and TTG1 regulate the same set of target genes (Fig. 4.2 and 4.3). It would not be surprising that TTG1 and GL3 regulate the same target genes in the trichome development pathway. To test this, I performed gene expression analysis on the direct trichome targets of GL3, including GL3, GL2, CPC and ETC1 (Fig. 2.3), by using a TTG1-GR inducible system. Our results show that GL2, CPC and ETC1 are also direct targets of TTG1, because the transcription of these genes increased significantly in response to TTG1-GR induction even in the absence of de novo protein synthesis. I have also identified TTG2 as a new immediate direct target of both TTG1 and GL3 (Fig. 3.2). TTG2 has been characterized as a WRKY transcription factor, which acts downstream of TTG1 and shares functions with GL2 in controlling trichome outgrowth (Johnson *et al*. 2002). These data show that TTG1 largely regulates the transcription of

the same regulatory loci as GL3 during trichome initiation. It also supports the *Not*Ion that TTG1 regulates the trichome pathway through affecting the activation capacity of bHLH proteins.

Interestingly, I failed to detect any changes in GL3 expression after TTG1-GR induction as opposed to the finding that GL3 is repressed by GL3-GR. It has been reported that GL3 binds to and activates GL2, CPC and ETC1 in a GL1-dependent manner but the GL3 self-repression is GL1-independent (Fig. 2.5). In our ChIP experiments with *gl1*/pGL1::GL1-YFP-cMYC, I detected the *in vivo* recruitment of GL1 to the CPC, ETC1, GL2 and TTG2 promoters but not to the promoter of GL3 (Fig. 3.2B). These data suggest that the GL1 DNA-binding activity is required for the TTG1-bHLH complex to select target genes. Additionally, the *in vivo* interaction between TTG1 and GL1 (Fig. 3.3B) fits perfectly with the model that TTG1, bHLH and MYB proteins form a TTG1-bHLH-MYB regulatory complex which is responsible for the activation of GL2, TTG2 and CPC. The TTG1-bHLH-MYB complex seems to only regulate the transcription of downstream targets but not the transcription of bHLH or R2R3-MYB proteins.

I could not detect changes in the expression of TRY and ETC2 by the induction of *gl3 egl3*/p35S::GL3GR (Fig. 2.3) or *ttg1*/p35S::TTG1GR (Fig. 3.2A). These results demonstrate that although TRY and ETC2 are largely redundant with CPC and ETC1, they are regulated differently, perhaps by GL2 for example, which is consistent with their different levels of expression in different tissues (Kirik *et al*. 2004b).

How does TTG1 function?

GL3 transcripts can be easily detected in the *ttg1* and *gl1* mutants (Payne *et al*. 2000) indicating that they are not required for GL3's transcription. I wanted to determine

whether TTG1 might regulate the subcellular location of GL3 the way that GL3 and EGL3 affect TTG1's location. In the *ttg1* mutant, I found that the GL3-YFP protein was still located entirely in the nucleus. But surprisingly, I found that the loss of TTG1 caused GL3 to be abnormally distributed within the nucleus of leaf epidermal cells. GL3 protein forms unevenly distributed "speckles" (Fig. 3.5A B). In contrast, the nuclear distribution pattern of GL1-YFP-cMYC in *ttg1* is very similar to the wild type pattern-more or less even nuclear distribution. I did find one or two GL1 speckles in a single nucleus (Fig. 3.5C). These results suggest that functional TTG1 protein is required for the appropriate bHLH distribution in the nucleus.

In *gl1* mutants, I detected a similar but even more severely speckled GL3-YFP distribution, specifically in the leaf epidermis (Fig. 3.4E-H). GL3 forms fewer but more clearly isolated nuclear speckles in *gl1* than in *ttg1*. I previously showed that in a *gl1* mutant, GL3 can no longer bind to the promoter of its major trichome targets, GL2 and CPC (Fig. 2.5B). Taken together, I conclude that GL1 is responsible for GL3 or the TTG1-bHLH complex tethering to the promoters of specific downstream targets, and TTG1 might function as a "helper" for the bHLH::GL1 interaction. Loss of proper DNA interactions leads to aberrant bHLH distribution-speckles. It will be important for future studies to provide direct molecular or biochemical evidence to confirm that TTG1 facilitates the interactions between bHLH and MYB proteins.

Besides participating in the TTG1-bHLH-MYB regulatory complex, TTG1 may regulate trichome genes through other mechanisms. In a recently published article, TTG1 physically interacts with GEM, a protein that modulates cell division and represses the expression of GL2 and CPC in *Arabidopsis* roots. Overexpression of GEM cause increased root hair and decreased leaf trichome densities (Caro *et al*. 2007). Overexpressed GEM proteins are shown to bind to the promoters of GL2 and CPC,

associated with the acquisition and/or maintenance of histone H3K9me2 (typical of silent heterochromatin regions) at these two genes. These data imply that the interaction between TTG1 and GEM could prevent GEM from joining a complex which represses the expression of GL2 and CPC or other trichome genes.

Trichome patterning

As discussed in the theoretical model (Meinhardt 1994; Meinhardt and Gierer 2000), *de novo* patterning requires the local self-enhancement of activators in combination with lateral inhibition by inhibitors. Based on this theory, a common model is proposed for the *Arabidopsis* trichome and root hair patterning, in which single MYB repressors (CPC and TRY) are thought to be able to move (faster than activators if activators can also move) into neighboring cells. The only evidence supporting this prediction is that although CPC-GFP proteins are expressed in non-root hair cell files, the CPC-GFP protein is also detected in the neighboring root hair files (Wada *et al*. 2002). In this paper, our microprojectile bombardment experiment with p35S::CPC-YFP directly demonstrates CPC's ability to move in leaf epidermis for the first time (Fig. 3.6), strongly supporting the current trichome patterning model from this perspective. CPC-YFP protein was detected in clustered epidermal cells up to two cells away from the bombardment center suggesting CPC could move from one cell to another (Fig. 3.6E). As I discussed, long-range repressors, CPC and possibly ETC1 (Kirik *et al*. 2004a), are directly activated by the TTG1-bHLH-MYB complex while the short-range repressor, TRY, is not. This may indicate that the TTG1-bHLH-MYB complex only activates long-range inhibition when it triggers the trichome pathway and the short-range inhibition might occur during later stages of trichome development.

In addition, I also tested the movement potential of TTG1, GL1 and GL2 and show that these proteins do not move in the leaf epidermis under the same condition where CPC moves. Another issue deserving special attention is that GL3 did not move from cell-to-cell in the leaf epidermis either, in contrast to the finding that GL3 moves between root cell files (Bernhardt *et al*. 2005). By examining the protein and Promoter::GUS expression patterns, I find that GL3 is transcribed in the trichome initial and surrounding epidermal cells where GL3 protein is not detectable (Fig. 3.7F). Therefore, the absence of GL3 protein in epidermal cells may not be caused by GL3 trafficking into developing trichomes, but rather by some form of posttranscriptional or translational modification.

The current model of trichome patterning is largely based on genetic analysis and molecular data obtained from the root hair system. The data presented in this paper has demonstrated that a similar molecular mechanism by a TTG1-bHLH-MYB regulatory complex directly activating downstream targets is responsible for trichome patterning. Based on this mechanism, I have refined the model for trichome patterning. As shown in Fig. 3.8, a functional activating complex TTG1-GL3/EGL3-GL1 activates activators (GL2 and TTG2) and single MYB repressors (CPC and ETC1) in the cell chosen to be a trichome. CPC and ETC1 will move into the neighboring cells where they, together with locally expressed repressors, compete with GL1's binding to EGL3 to form an inactivating complex TTG1-EGL3-CPC/ETC1. This inactivating complex disrupts the function of the activating complex, TTG1-EGL3-GL1. The decreased concentration of TTG1-EGL3-GL1 in these epidermal cells is not enough to activate GL2 and TTG2 beyond a required threshold level and the trichome cell fate is not triggered.

Our results have also shown differences between the trichome and root hair pathways at the molecular level: (1) GL3 is preferentially transcribed in the cells where it

functions during trichome development, while GL3 is transcribed in non-root hair cell files and accumulates and functions in root hair cell files during root hair patterning; (2) GL3 does not move in the leaf epidermis but it moves in the root epidermis. This raises many new questions for this regulatory network. Identification of the molecular components which mediate the differentiation of bHLH expression patterns in different tissues will allow the study of how these key developmental complexes are regulated in the plant.

Figure 3.1: Expression pattern of YFP-TTG1 fusion in the leaf epidermis.

Maximum intensity projection images of confocal stacks of a TTG1::YFP-TTG1 construct in developing leaves of 20-day-old *ttg1* mutant seedlings. **A**. Overview of a developing leaf, which is not flat so that in some areas the pavement cells are in focus and in other areas, focus is higher up on the trichomes. **B**. Branching trichomes. **C** Trichome initials (arrow). Bars in A = 100um; B = 50um; C = 10um.

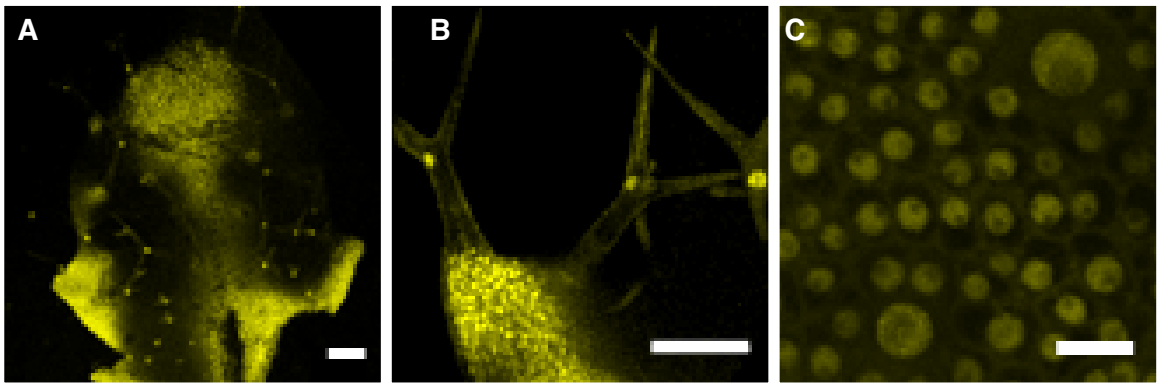

Figure 3.2: Direct activation of GL3 target genes by TTG1-GR.

A, Gene expression level was measured by Relative Quantitative RT-PCR. The results were calculated with comparative Ct method (ABI bulletin) and presented as fold changes compared to the mock or cyclohexamide treatment, which were standardized by the constitutive expression level of ACTIN gene. The induced gene expression levels were statistically significant against those of control treatments ($P<0.05$); error bar indicates range of expression change. **B**. Semi-quantitative PCR of ChIP experiments carried out with chromatin obtained from green tissues of 20 days-old *gl1*/pGL1::GL1-cMYC-YFP (left), or *ttg1*/pTTG1::YFP-TTG1 (right) plants. PCRs were performed on three four-fold serial dilutions of the ChIP-ed material, represented by the black slope on the top. Although ETC1 is directly transcriptionally activated by TTG1, I can not detect TTG1 binding to the ETC1 promoter. This may be due to technical problems (Asterisk).

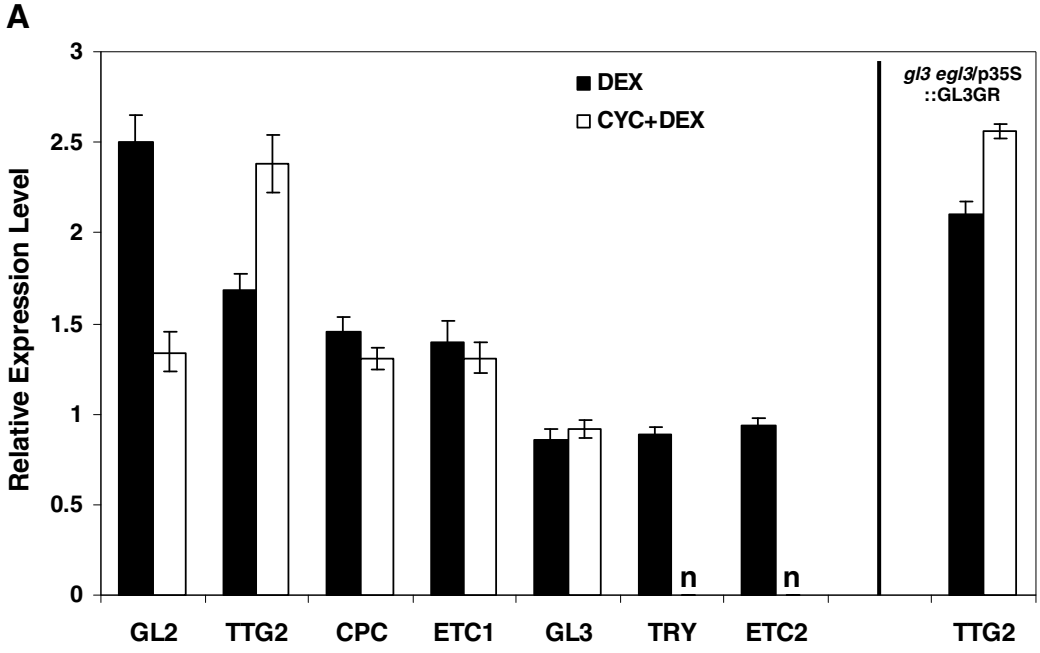

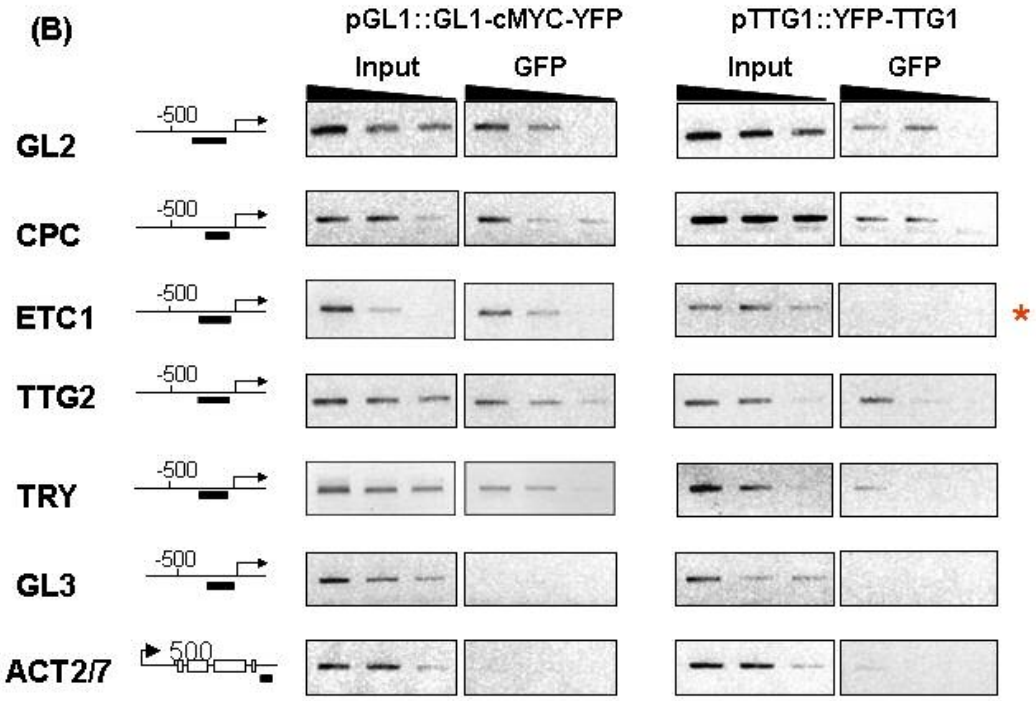
(B)
pGL1::GL1-cMYC-YFP
pTTG1::YFP-TTG1
Input
GFP
Input
GFP
GL2
CPC
ETC1
TTG2
TRY
GL3
ACT2/7
-500
-500
-500
-500
-500
-500
500
*

Figure 3.3: Co-precipitation of TTG1-cMYC With HA-GL3-6His and GL1-YFP-6His from seedling extracts.

Crude protein extracts were precipitated with His-Select Ni columns. Aliquots of the input extracted proteins and elution fractions from Ni columns were separated by 4-12% SDS gels, blotted and probed with anti-myc 9E10 mAb (IP: protein input; HE: elution from His-Select column). **A**, Lane 1, 4:TTG1-cMYC; lane 2, 5: HA-GL3-6His; lane 3, 6: TTG1-cMYC/HA-GL3-6His. **B**, Lane 1, 4:TTG1-cMYC; lane 2, 5: GL1-YFP-6His; lane 3, 6: TTG1-cMYC/GL1-YFP-6His.

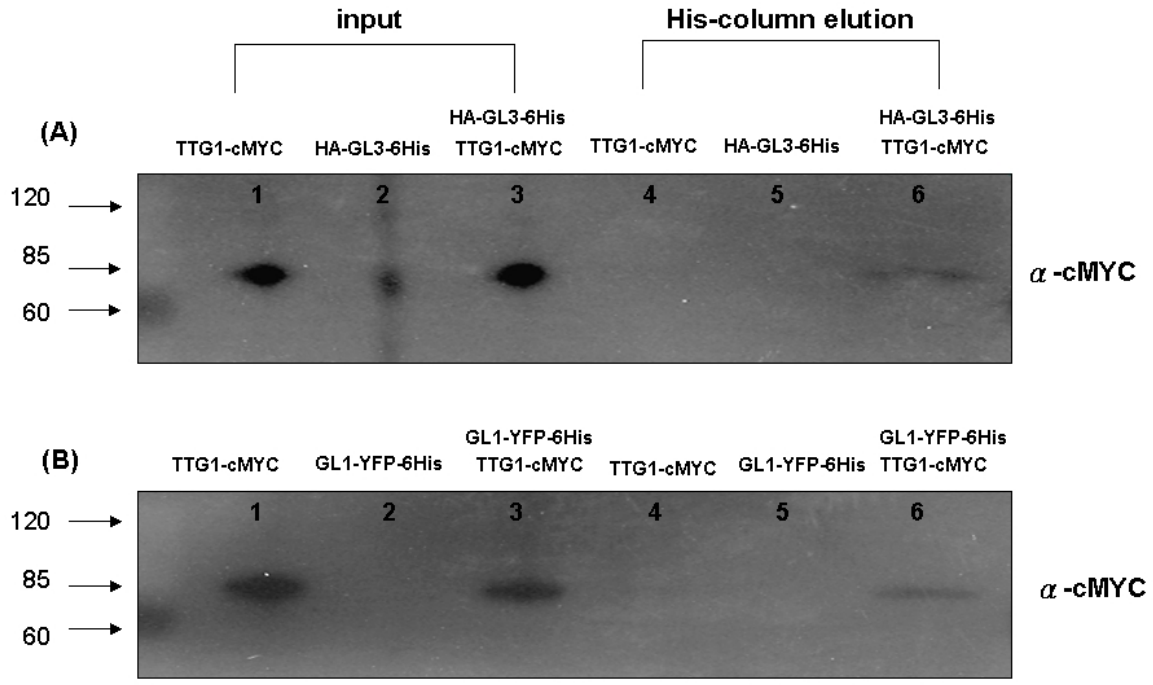

Figure 3.4: Increased level of cytoplasmic TTG1 in the epidermal cells of *gl3 egl3* mutant plants .

A-D, Maximum intensity projection images of confocal stacks of TTG1::YFP-TTG1 and GL1::GL1-YFP-cMYC in leaf epidermal cells of 20-day-old seedlings. More than five independent transformant have been examined and the pictures were taken with leaves from representative plants. Significant YFP-TTG1 signal was observed in the *gl3 egl3* cytoplasm (compare A and B). Bar = 10 um. **E**, Quantification of ratio (cytoplasm/total) fluorescence. Error bar represents standard error.

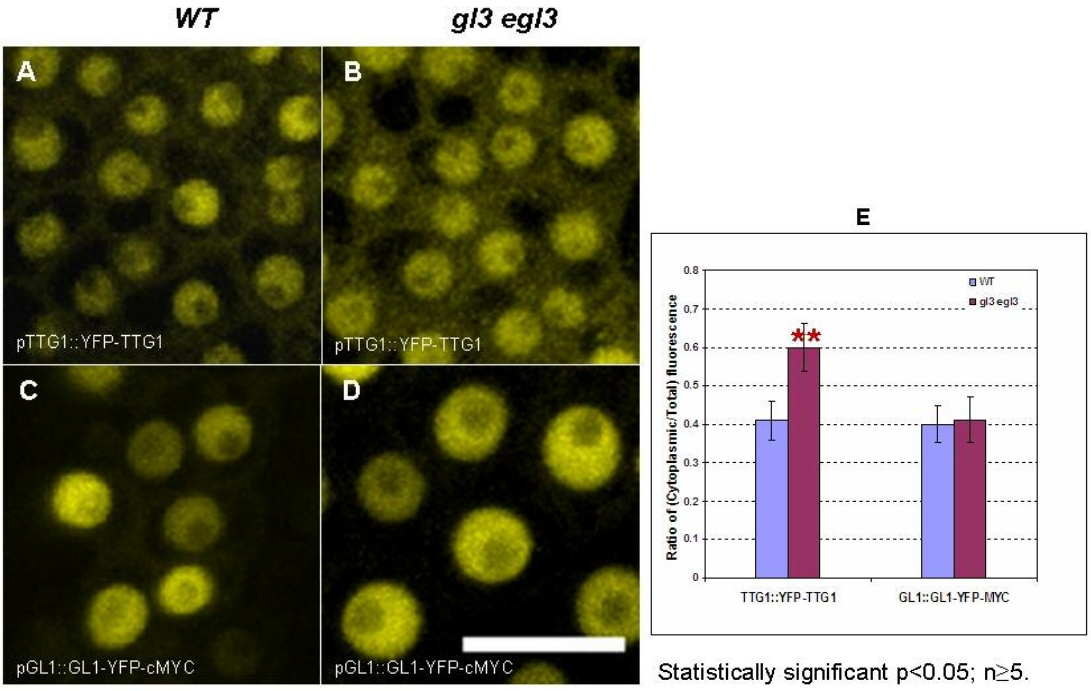

Figure 3.5: GL3 forms speckles in the epidermal cells of *ttg1* and *gl1* mutant plants.

Maximum intensity projection images of confocal stacks of GL3-YFP and GL1-YFP in leaf epidermal cells of 20-day-old *ttg1* (A-D) and *gl1* (E-H) mutant seedlings. A, B, E and F: GL3-YFP is unevenly distributed and formed speckles. C and D: GL1-YFP formed only a couple of speckles in nuclei in occasional cells. G and H: uniform GL3-YFP distribution in root epidermal cells. Bar = 10 um.

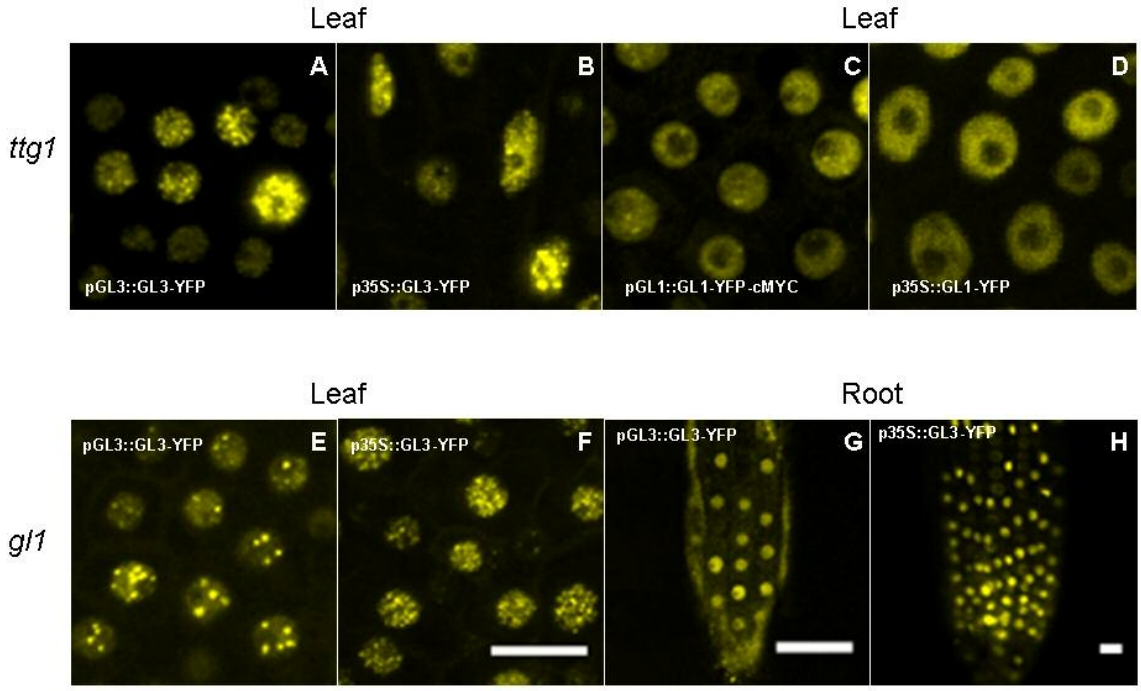

Figure 3.6: Intercellular trafficking of CPC-YFP fusion protein after microprojectile bombardment.

Maximum intensity projection images of confocal stacks bombarded *gl3 egl3* leaf epidermal cells. YFP fluorescence is green (A-E), and background chlorophyll autofluorescence is red (F-J).YFP and chlorophyll integrated (K-O). CPC-YFP (D) shows extensive cell-to-cell movement to a cluster of approximately 10 epidermal cells and is present throughout the cytoplasm and nucleoplasm. TTG1 (A), GL3 (B), GL1 (C) and GL2 (E) YFP fusions are cell autonomous, as fluorescence is restricted to single cells. Bar = 10 um.

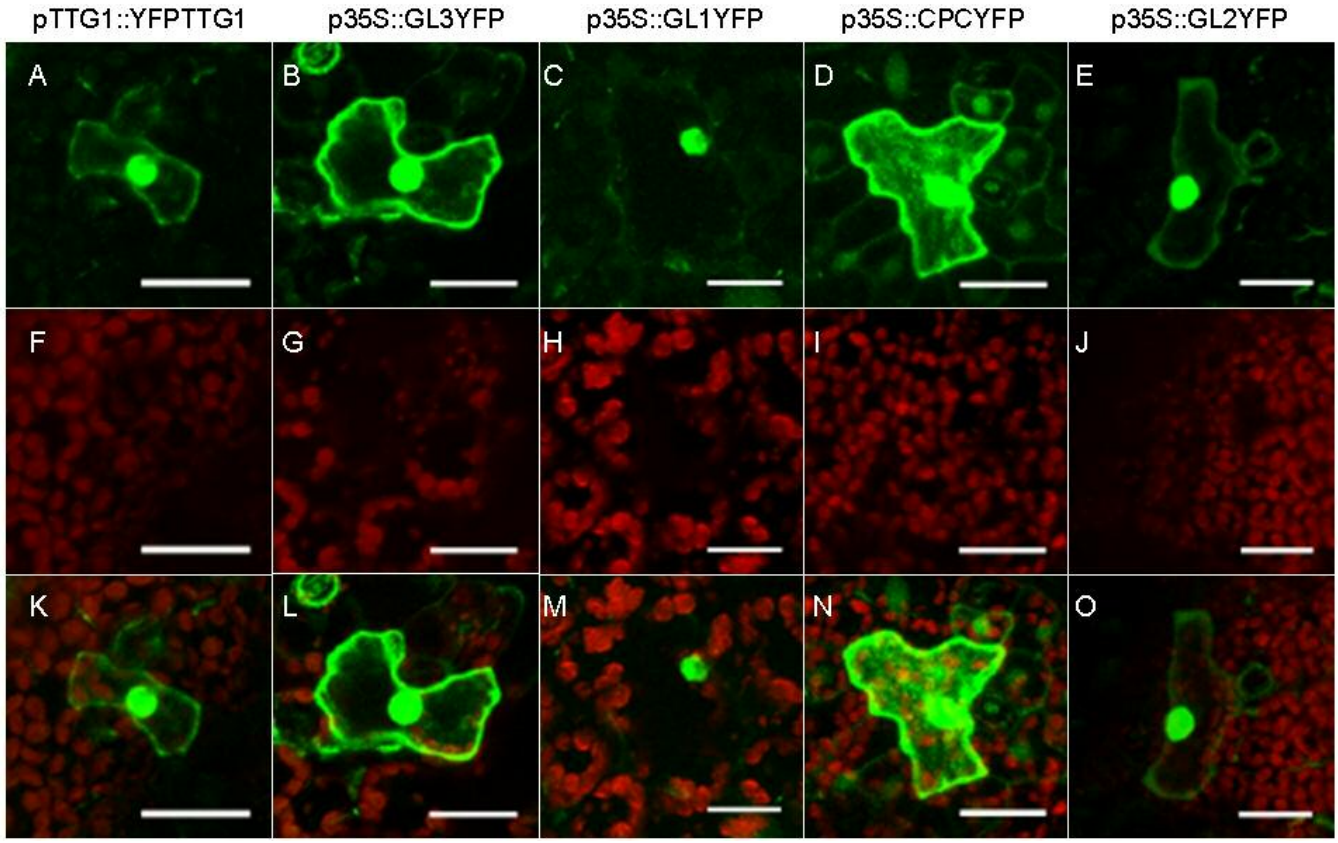

Figure 3.7: The transcription and protein expression pattern *GL3* and *EGL3* in the leaf epidermis.

A-D. Analysis of *GL3* and *EGL3* promoter activity in the wild-type (WT) leaves using *GL3::GUS* and *EGL3::GUS* reporter lines. *GL3 (A and B)* and *EGL3* (C and D) are transcribed in trichomes and neighboring cells. E and F. Accumulation of pGL3::GL3YFP only in trichomes of *gl3* mutant leaves. G and H. pEGL3::EGL3YFP was expressed in both trichomes and pavement cells of *gl3 egl3* mutant leaves. Arrows indicate active trichome initiation. Bar (E and G) = 100um; Bar (F and H) = 20um.

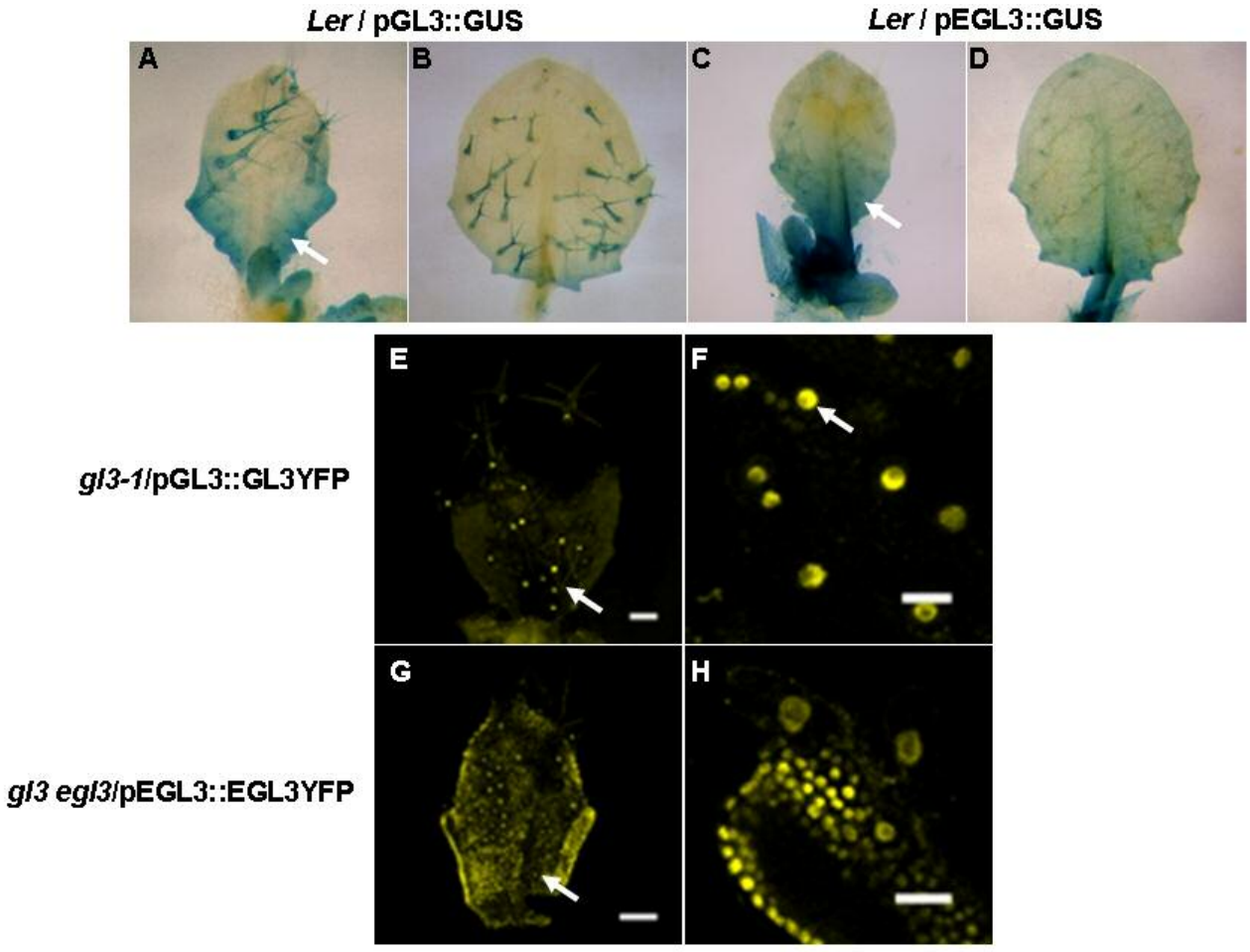

Figure 3.8: Modified model for *Arabidopsis* trichome initiation and patterning.

Regulators of trichome fate are depicted in green shades, activators (GL2/TTG2) is in yellow and inhibitors (CPC/ETC1) are in orange. Arrows indicate transcriptional activation. In trichome cells the inhibitors are directly activated by the activating complex and move (dashed lines) into neighboring cells, where they and endogenous inhibitors block (red) the activity of the activating complex thereby decreasing the expression of GL2/TTG2 to below a required threshold level (dashed arrows). Therefore, the trichome cell fate is not triggered.

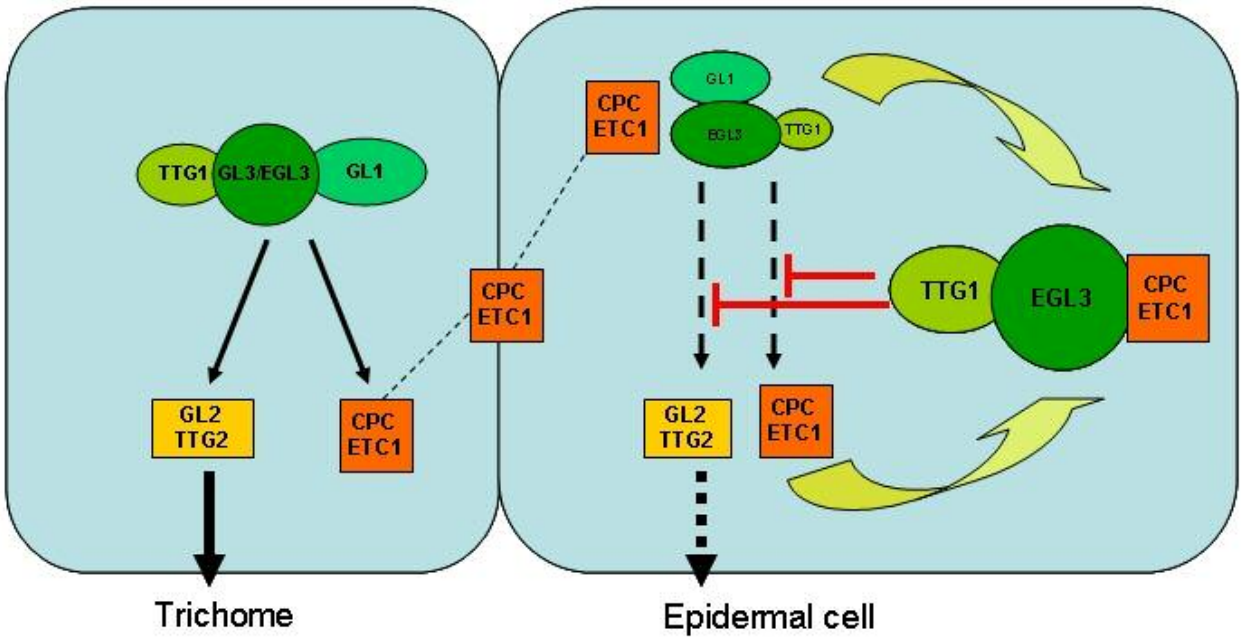

Chapter 4: Regulation of the anthocyanin biosynthetic pathway in *Arabidopsis* seedlings

INTRODUCTION

The role of the TTG1-bHLH-MYB complex in regulating trichome development has been explored in previous chapters. However, specific combinations of this complex also regulate the branch of the phenylpropanoid pathway yielding flavonoid-based pigments. In plants this pathway has proven to be an excellent model for the study of transcriptional regulation. Flavonoid pigment biosynthetic genes are regulated developmentally and in response to various biotic and abiotic stresses by a combination of transcription factors. These transcriptional regulators include members of the Myb, bHLH and WD-repeat families (Taylor and Briggs 1990; de Vetten *et al*. 1997; Quattrocchio *et al*. 1999; Walker *et al*. 1999; Spelt *et al*. 2000; Zhang *et al*. 2003; Carey *et al*. 2004; Morita *et al*. 2006; Schwinn *et al*. 2006). Different transcription factor combinations can specify the class of flavonoid pigment produced, where it will be produced, production in response to a particular stimulus, and whether transcriptional regulation of structural genes is positive or negative (Taylor and Briggs 1990; Burr *et al*. 1996; Aharoni *et al*. 2001; Winkel-Shirley 2001; Piazza *et al*. 2002; Baudry *et al*. 2004; Hartmann *et al*. 2005; Lepiniec *et al*. 2006; Solfanelli *et al*. 2006).

This model for the transcriptional regulation of the flavonoid pigment pathway first emerged over 20 years ago with the very first cloning of a plant transcription factor, an R2R3 Myb from maize (Zea maize) known as colorless1 (c1) (Cone *et al*. 1986; Paz-Ares *et al*. 1987). Shortly after the cloning of c1, bHLH transcription factors, such as r, were identified that regulate flavonoid pigment production in parallel with the Myb

proteins (Ludwig *et al*. 1989; Chandler *et al*. 1989; Goff *et al*. 1992). Since then, this general WD repeat-Myb-bHLH model for the regulation of the anthocyanin biosynthetic pathway was found to be operating in all higher plant species studied including snapdragon (Antirrhinum majus), petunia (Petunia hybrida), and *Arabidopsis* thaliana (de Vetten *et al*. 1997; Quattrocchio *et al*. 1999; Walker *et al*. 1999; Spelt *et al*. 2000; Zhang *et al*. 2003; Morita *et al*. 2006; Schwinn *et al*. 2006). Moreover, based (partly) on the genes regulated by the myb-bHLH transcriptional complex the flavonoid biosynthetic pathway is divided into "early" and "late" steps. The late pathway genes defined by their dependence on Mybs and bHLHs for their expression, while the early genes are not (Martin *et al*. 1991; Quattrocchio *et al*. 1993; Shirley *et al*. 1995; Pelletier and Shirley 1996; Pelletier *et al*. 1997; Zhang *et al*. 2003).

Despite the wealth of knowledge regarding the WD-bHLH-Myb regulatory model governing not only the phenylpropanoid pathway in many plant species but also various cell fate pathways in *Arabidopsis* (previous chapters; Lee and Schiefelbein 1999; Payne *et al*. 2000; Winkel-Shirley 2001; Bernhardt *et al*. 2003; Bernhardt *et al*. 2005; Zhang *et al*. 2003; Lepiniec *et al*. 2006; Serna and Martin 2006), little is known about anthocyanin pathway regulation with respect to targets of TTG1-dependent complexes and relative contributions of specific bHLH and myb transcription factors to structural gene regulation. Recently the Production of Anthocyanin Pigment1 (PAP1) myb has been shown to be an anthocyanin regulator in seedlings (Teng *et al*. 2005). However, three other *Arabidopsis* Myb candidates (PAP2, Myb113 and Myb114) exist based on several criteria: sequence similarity to PAP1 and pigment regulators of other plant species, on their ability to interact with *Arabidopsis* bHLH anthocyanin regulators Glabra3 (GL3), Enhancer of Glabra3 (EGL3) and Transparent Testa8 (TT8) in yeast, and, in the case of PAP2, its ability to up-regulate the phenylpropanoid pathway when overexpressed

(Borevitz *et al*. 2000; Stracke *et al*. 2001; Zhang *et al*. 2003; Zimmermann *et al*. 2004; Fig. 1). PAP1 and PAP2 were originally identified through activation tagging experiments, with plants overexpressing either of these Mybs showing dramatic increases of anthocyanin pigment. This increase in flavonoid pigment production is due to the up-regulation of the entire phenylpropanoid pathway as evidenced by increases in late structural gene expression and more modest increases in early structural gene expression in PAP1 overexpressing leaves (Borevitz *et al*. 2000; Tohge *et al*. 2005a). This observation is curious as it suggests that myb/bHLH/TTG1 transcriptional complexes in *Arabidopsis* possibly regulate more than just a late subset of flavonoid pathway genes, contrary to pathway regulation by bHLHs and Mybs in other plant species.

EGL3, GL3 and *TT8* have previously been identified as regulators of anthocyanin pigment production. Mutant phenotype analysis in young seedlings demonstrates a minor role for *GL3* with greater contributions made by *EGL3*. Limited anthocyanin structural gene expression studies in seedlings show down regulation of the late gene *dihydroflavonol reductase* (*DFR*) but not the early gene *chalcone synthase* (*CHS*) in *gl3 egl3* and *gl3 egl3 tt8* multiple mutants (Zhang *et al*. 2003). Gene expression studies in developing siliques of proanthocyanidin (PA; seed coat condensed tannins)-deficient tt8 (and tt2 myb) mutants also demonstrate regulation of only late flavonoid genes with both *TT8* and *TT2* directly regulating the PA-specific structural gene *Banyuls* (*BAN*) (Nesi *et al*. 2000; Nesi *et al*. 2001; Baudry *et al*. 2004). Interestingly, *TT8* has been shown to auto-regulate, being a direct target of TTG1-dependent complexes in developing siliques (Baudry *et al*. 2006).

In this chapter I attempt to better understand flavonoid pathway regulation by Myb/bHLH/TTG1 transcriptional complexes of *Arabidopsis*. Studies utilizing 35S:GL3:GR and 35S:TTG1:GR fusions in seedlings reveal late anthocyanin

biosynthetic genes as direct targets of TTG1-dependent transcriptional complexes but uncover no regulation of early biosynthetic genes. In addition, GL3:GR studies in single and multiple bHLH mutant seedlings molecularly confirms a greater contribution by EGL3 than by GL3 in anthocyanin structural gene regulation as first evidenced by mutant phenotype analysis (Zhang *et al*. 2003).

MATERIAL AND METHODS

Arabidopsis Accessions

gl3 egl3/p35S::GL3GR and ttg1/p35S:TTG1GR were previously described in chapter 2. Transgenic plant *gl3 EGL3*/p35S::GL3GR was created by transformation of *gl3* mutant plants followed by screening for BASTA resistance.

Flavonoid biosynthetic gene expression in GL3::GR and TTG1::GR transgenics

QPCRs with *gl3 egl3*/p35S::GL3GR and *ttg1*/p35S:TTG1GR were performed as described in chapter 3.

RESULTS:

Direct Regulation of Late Flavonoid Biosynthetic Genes by the TTG1-Dependent Transcriptional Complex

To better define the flavonoid biosynthetic gene set regulated by TTG1/bHLH/Myb transcriptional complexes *GL3* and *TTG1* genes were fused to the glucocorticoid receptor (Lloyd *et al*. 1994; Baudry *et al*. 2006) and placed under the control of the cauliflower mosaic virus 35S promoter. These fusion proteins,

constitutively expressed in plants, are inactive without dexamethasone (DEX) treatment. Addition of DEX allows the chimeric transcription factors to regulate their primary and secondary targets. Simultaneous treatment with DEX and cycloheximide (CHX) blocks *de novo* protein synthesis, allowing the identification of primary targets only (Sablowski *et al*. 1998). Recovery of *gl3 egl3* double mutant and *ttg1* mutant by GL3::GR and TTG1::GR fusions, respectively, indicated that these chimeric proteins are functional (Fig. 4.1; Baudry *et al*. 2004).

35S:GL3:GR transgenic *gl3 egl3* seedlings were assayed by QPCR for gene expression changes after DEX induction for a range of flavonoid biosynthetic and regulatory genes including *PAL1, CHS, CHI, FLS1, F3H, F3'H, DFR, LDOX, GST12, TTG1, TT8, EGL3, PAP1* and *PAP2*. This experiment identified the structural genes *F3'H, DFR, LDOX,* and the regulatory genes *TT8* and *PAP2* as up-regulated by GL3 overexpression (Fig. 4.2). The experiment was repeated with a DEX plus CHX treatment to determine if any of these loci are directly regulated by GL3. All three structural genes again were up-regulated in response to GL3::GR induction (Fig. 4.2). Also, TT8 was directly up-regulated by GL3, consistent with the findings of Baudry *et al*. (2006) identifying TT8 as a direct target of TT2 and TTG1. Interestingly, PAP2 appears to be a secondary target of GL3.

35S:TTG1:GR transgenic *ttg1* seedlings were similarly analyzed for expression changes in flavonoid biosynthetic and regulatory genes after DEX induction. Genes tested included *CHS, CHI, F3H, F3'H, DFR, LDOX, GST12, TT8, EGL3, PAP1* and *PAP2*. DEX induction of TTG1:GR resulted in the up-regulation of *F3'H, DFR, LDOX* and *TT8* in transgenic *ttg1* seedlings (Fig. 4.3). Induction with DEX plus CHX identified *DFR, LDOX* and (as previously shown in Baudry *et al*. 2006) *TT8* as direct targets of

TTG1. Although identified as a direct target of GL3, *F3'H* in this case appears to be a secondary target of TTG1.

GL3 and EGL3 differentially regulate late flavonoid biosynthetic genes

I next determined the effects on gene regulation by DEX induction in *35S:GL3:GR* transgenic *gl3* single vs. transgenic *gl3 egl3* double mutants to gain further insight into the mechanisms of flavonoid gene regulation by TTG1/bHLH/Myb transcriptional complexes. Genes tested included *TTG1, TT8, F3'H, DFR* and *LDOX* and any expression changes in these genes reported as fold increases relative to gene expression in mock-treated *35S:GL3:GR* transgenic *gl3 egl3* seedlings.

TT8 is expressed to higher levels in un-induced gl3 mutant seedlings than in DEX-induced gl3 egl3 double mutant seedlings, suggesting that EGL3 contributes more to TT8 regulation than GL3 even when GL3 is overexpressed (Fig. 4.4). Moreover, TT8 expression is highest in DEX-induced *gl3* single mutant seedlings (to about double the levels in DEX-induced double mutant and un-induced single mutant seedlings), suggesting that both GL3 and EGL3 can additively contribute to the regulation of TT8. Similarly, F3'H reaches highest expression levels in DEX-induced *gl3* single mutant seedlings with only about half as much expression observed in DEX-induced double mutant and un-induced *gl3* single mutant (Fig. 4.4). Again, this suggests additive effects by these bHLH proteins for F3'H regulation with perhaps greater contribution by EGL3 considering that GL3 is driven by a strong promoter.

Interestingly, the results of this experiment with respect to DFR and LDOX suggest a different mechanism for the regulation of these genes over TT8 and F3'H. For either DFR or LDOX, highest expression is achieved in both un-induced and DEX-induced *gl3* single mutant seedlings (Fig. 4.4); overexpressing GL3 has no effect as long

as the wild-type EGL3 locus is present. This suggests a greatly reduced role for GL3 in DFR and LDOX regulation, consistent with the observation that fold increases in DEX-induced over un-induced double mutant seedlings for DFR and LDOX are only about half as high as increases observed for TT8 and F3'H in the double bHLH mutant.

DISCUSSION

Despite being a heavily studied pathway in the most intensely studied plant molecular genetic model, the genes that are regulated by TTG1-dependent Myb/bHLH transcriptional complexes during anthocyanin production in *Arabidopsis* are still being identified and characterized. In this study, biosynthetic gene expression studies in seedlings overexpressing GL3:GR or TTG1:GR reveal late flavonoid biosynthetic genes as direct targets with no early gene up-regulation observed in response to GL3 or TTG1 overexpression. I also show that GL3 and EGL3 differentially regulate these flavonoid biosynthetic target genes.

The TTG1-dependent anthocyanin Mybs of *Arabidopsis* specifically regulate the late anthocyanin pathway genes beginning with *F3'H*

It can be noted that, where examined, genes of the phenylpropanoid pathway before *CHS* (such as *PAL*, *C4H* and *4CL*) are not down-regulated in *ttg1* or *ttg1*-dependent regulatory mutants. For example, flowers of the *Antirrhinum del* bHLH regulatory mutant do not show a reduction in *PAL* expression (Martin *et al*. 1991). Similarly, *Petunia an1* bHLH, *an2* Myb and *an11* WD-repeat mutant flowers show PAL expression levels comparable to wt (Quattracchio *et al*. 1993). In *Arabidopsis*, developing siliques of *tt8* and *ttg1* mutant plants express wild-type levels of *C4H* (Nesi *et al*. 2000),

while *tt8* and *ttg1* mutant seedlings express normal levels of *PAL* (Winkel-Shirley *et al*. 1995). Yet the observation exists that *PAP1* overexpression results in the up-regulation of genes across the entire phenylpropanoid pathway including genes such as *PAL1* (Borevitz *et al*. 2000; Tohge *et al*. 2005a). Without analysis of loss-of-function mutants, however, the question remained whether the *Arabidopsis* mybs are such broad regulators of the phenylpropanoid pathway. Given the observations made in the *Arabidopsis* multiple-myb knock-down and *pap1* insertion mutants it appears that these mybs in *Arabidopsis* are regulators of late anthocyanin structural genes (beginning at *F3'H*) (Gonzalez *et al*., 2007).

It is possible that PAP1 and/or TTG1-dependent transcriptional complexes when in excess have the ability to directly regulate early flavonoid genes, explaining the observations made in *pap1-D* plants. Alternatively, late anthocyanin pathway genes may be the direct targets of Myb/bHLH/TTG1 complexes in *Arabidopsis* with any early gene expression changes observed in *pap1-D* due to secondary effects or some metabolite feedback phenomenon resulting from the dramatic up-regulation of late pathway genes and increased flux through the flavonoid pathway (Jorgensen *et al*. 2005); at least at the protein level it has been shown that decreasing the activity of the later part of the pathway as in *tt3* and *ttg1* mutants can alter levels of early flavonoid enzymes (Pelletier *et al*. 1999). The observation that early gene expression is not responsive to *GL3* or *TTG1* overexpression together with the observations that early gene expression in response to *PAP1* overexpression does not seem to reliably increase in all instances and organs examined (leaves, seedlings and roots) that still over-accumulate pigment suggests that these transcription factors do not regulate early flavonoid biosynthetic genes.

Interestingly, while the expression of other late genes such as DFR and LDOX is nearly off/undetectable in *ttg1* and strong bHLH loss-of-function mutants (Winkel-

Shirley *et al*. 1995; Pelletier *et al*. 1997; Zhang *et al*. 2003; Gonzalez *et al*., 2007), F3'H expression is as high as 30% of wild-type in strong bHLH loss-of-function multiple mutant seedlings. This suggests that F3'H may be dually regulated by TTG1-dependent and independent mechanisms, consistent with its requirement for both the production of quercetin-based flavonols and cyanidin-based anthocyanins.

The Myb/bHLH/WD-repeat transcriptional complex regulates late structural genes of the anthocyanin pathway in many plant species

An interesting question of biological relevance regarding PAP Myb function is whether observations made in PAP1 overexpressors accurately reflect phenylpropanoid pathway regulation by the PAP Mybs in *Arabidopsis*. If it does this would be contrary to pathway regulation by orthologous Mybs in other plant species where the anthocyanin pathway has been examined; in all cases only a subset of the phenylpropanoid pathway genes are affected by loss-of-function mutations in Myb or bHLH regulatory loci. However, the particular set of genes can differ between species and between tissues within a species (Fig. 4.5). For example Antirrhinum Myb and bHLH mutants show down-regulation of structural genes beginning with F3H (Martin *et al*. 1991; Schwinn *et al*. 2006), while Myb and bHLH anthocyanin regulators in *Arabidopsis* regulate at F3'H (this study). In Petunia anthocyanin gene regulation by An1 bHLH and An2 Myb begins with DFR (Quattrocchio *et al*. 1993; Brugliera *et al*. 1999). Similarly it was recently shown that a pepper anthocyanin Myb mutant does not express DFR or LDOX but does express CHS to wild-type levels (Borovsky *et al*. 2004). Interestingly, in maize kernels the Myb/bHLH transcriptional complex coordinately regulates genes of the flavonoid pathway beginning with *CHS* but in maize seedlings, expression of *F3H* and *DFR* but not *CHS* requires a functional *R* bHLH allele (Taylor and Briggs 1991; Deboo *et al*. 1995).

Ipomoea myb1/c-1 and *wdr1/ca* mutants were recently shown to be down-regulated for genes of the flavonoid pathway beginning with *CHS* similar to structural gene regulation in maize kernels but in contrast to gene regulation observed in other dicots (Morita *et al*. 2006). Interestingly, these authors still note a regulatory difference between early and late biosynthetic genes with respect to *MYB1/C-1* and *WDR1/Ca*; the early genes examined (*CHS*, *CHI* and *F3H*) show expression levels 10-20% of wild-type while late genes (*F3'H*, *DFR*, *LDOX*, *3GT*, *3GGT* and a *GST*) are undetectable. Thus a general trend may be noted across all the plant species studied in which a WD-repeat/Myb/bHLH transcriptional complex predominantly regulates late genes over early genes, with the particular pathway steps comprising late and early sets and the degree of regulation of the sets differing between species and tissues (Fig. 4.5).

Figure.4.1: Recovery of anthocyanins in *gl3 egl3* seedlings expressing GL3:GR

A. mock-treated *gl3 egl3* transgenic seedlings. B. DEX-treated *gl3 egl3* transgenic seedlings

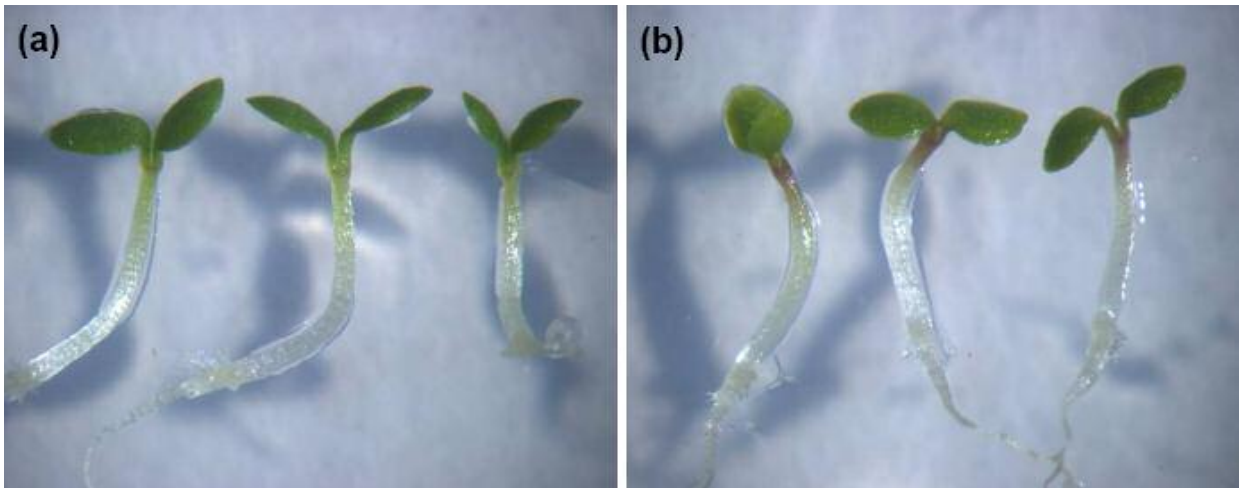

Figure 4.2: Anthocyanin gene expression in *gl3 egl3* mutant seedlings expressing GL3::GR.

Expression changes in DEX-treated and DEX-plus-CHX-treated plants reported as fold increases compared to mock treatment. Error bar indicates range of expression change.

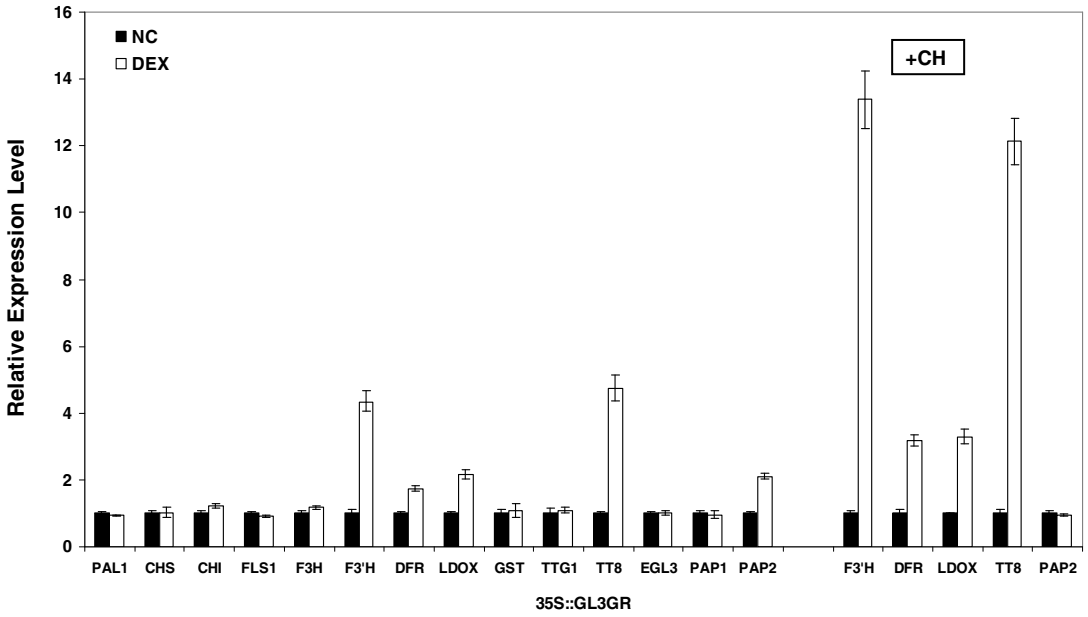

Figure 4.3: Anthocyanin gene expression in *ttg1* mutant seedlings expressing TTG1::GR.

Expression changes in DEX-treated and DEX-plus-CHX-treated plants reported as fold increases compared to mock treatment. Error bar indicates range of expression change.

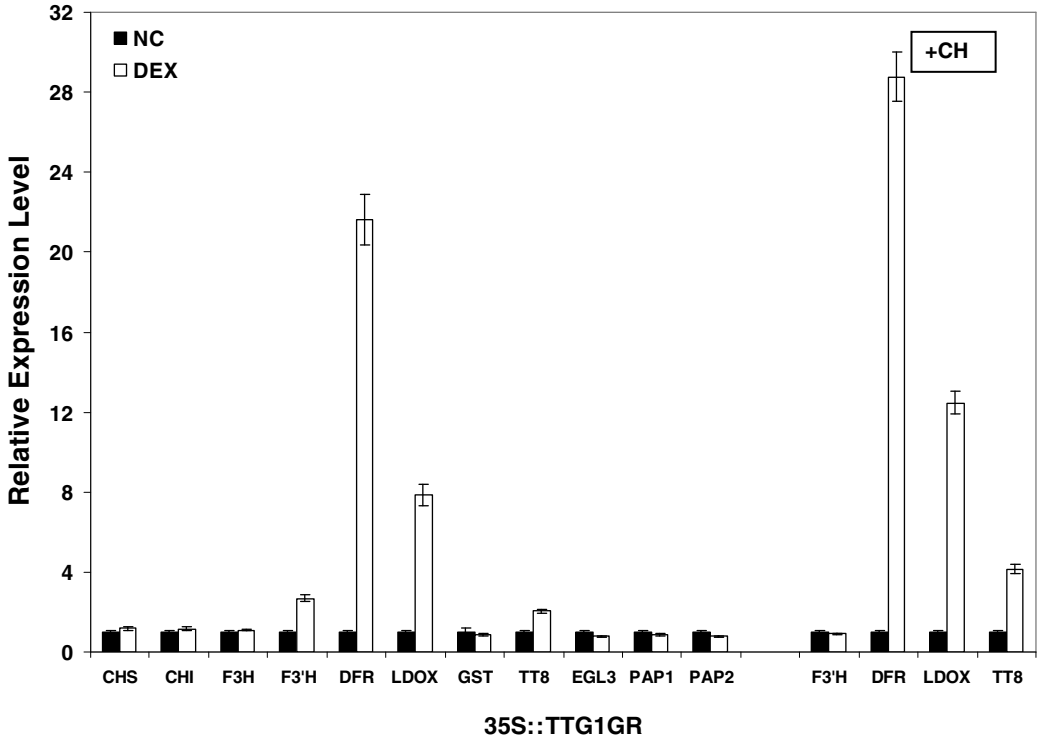

Figure 4.4: Anthocyanin gene expression in *gl3* and *gl3 egl3* mutant seedlings expressing GL3::GR.

Expression changes in reported as fold increases. Error bar indicates range of expression change.

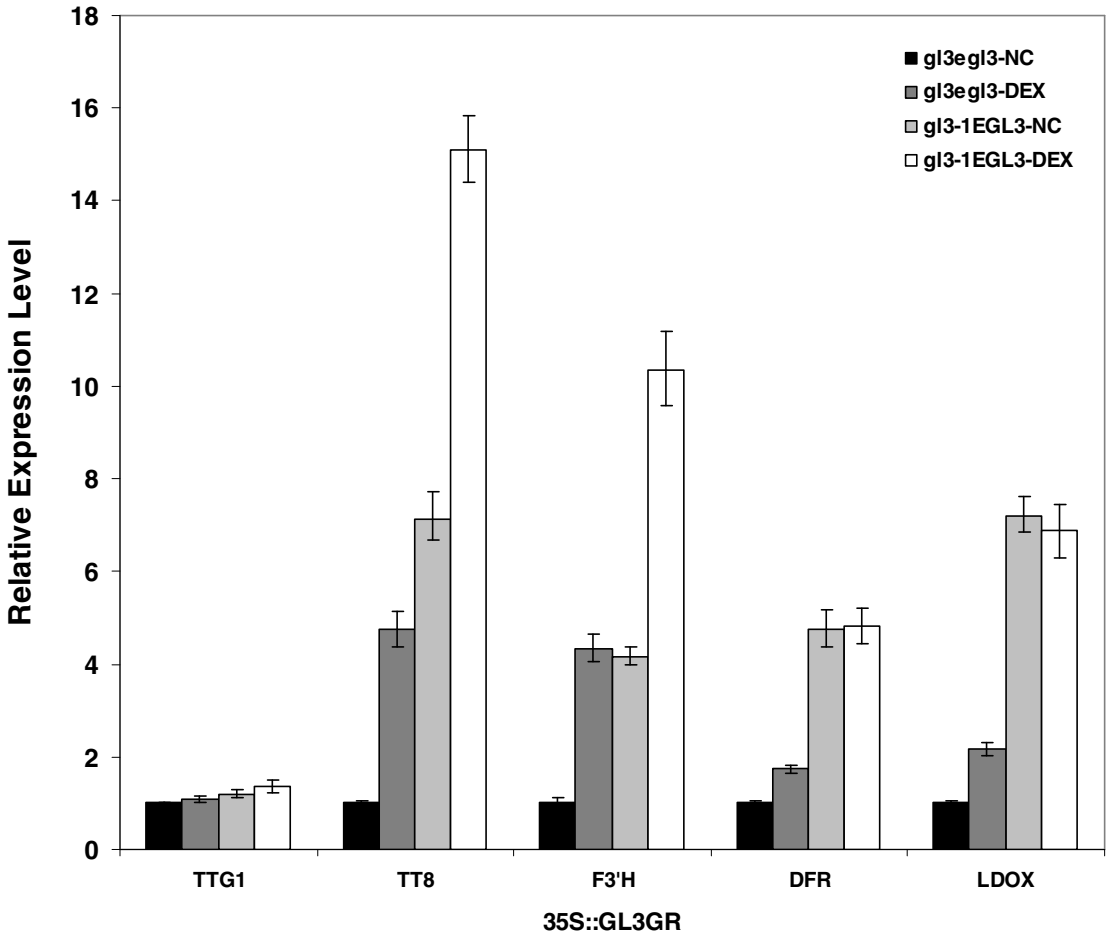

Figure 4.5: The branch of the phenylpropanoid biosynthetic pathway yielding anthocyanins.

Brackets indicate early and late divisions of the flavonoid pathway in *Arabidopsis* with the late genes regulated by Myb, bHLH, and WD-repeat proteins. Thin horizontal arrows indicate the first structural gene in the pathway regulated by Myb/bHLH/WD-repeat transcriptional complexes in other plant species.

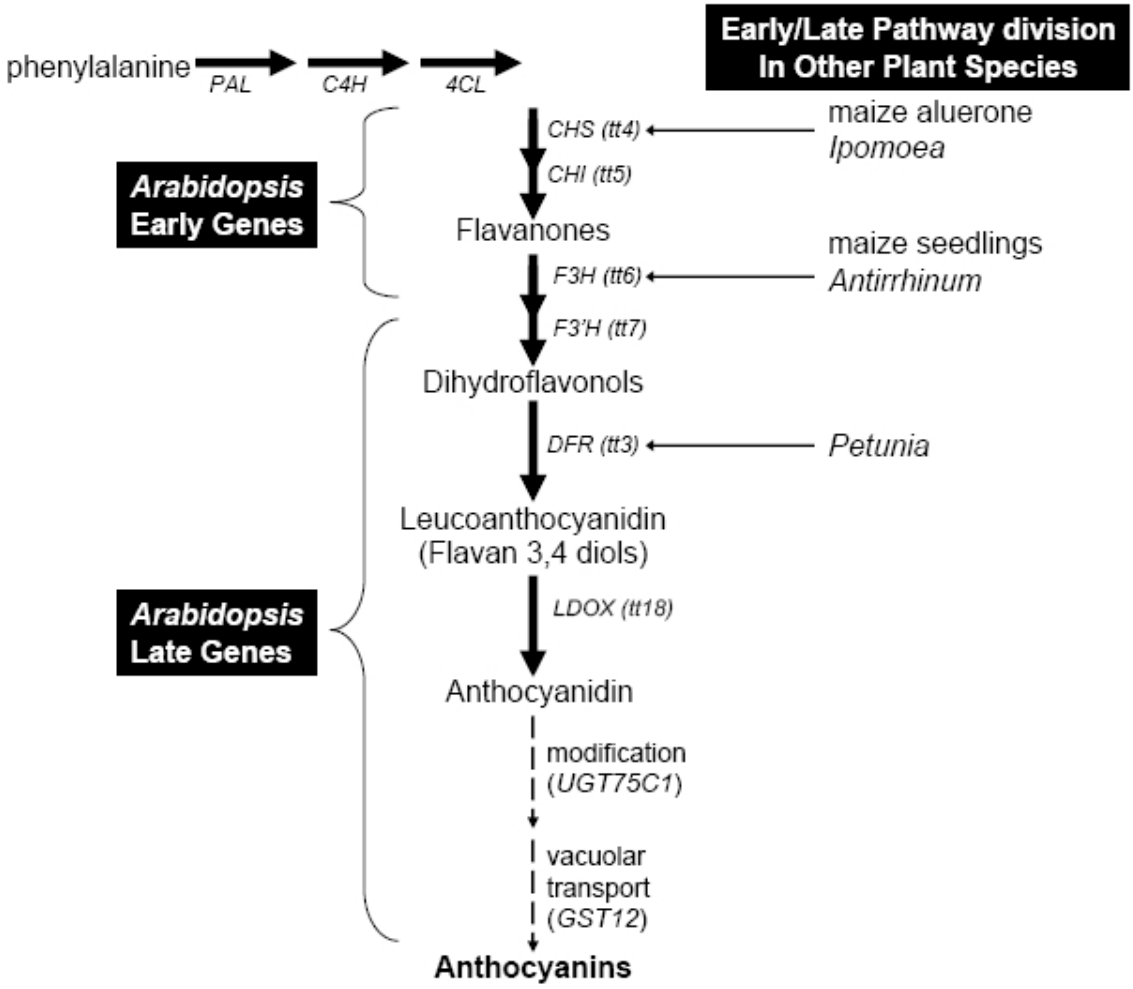

Bibliography

Aharoni, A., De Vos, C. H. R., Wein, M., Sun, Z., Greco, R., Kroon, A., Mol, J. N. M. and O'Connell, A. P. (2001). The strawberry FaMYB1 transcription factor suppresses anthocyanin and flavonol accumulation in transgenic tobacco. Plant J. 28, 319-332.

Baudry, A., Heim, M.A., Dubreucq, B., Caboche, M., Weisshaar, B., and Lepiniec, L. 2004. TT2, TT8, and TTG1 synergistically specify the expression of BANYULS and proanthocyanidin biosynthesis in *Arabidopsis* thaliana. Plant J 39(3): 366-380.

Baudry, A., Caboche, M. and Lepiniec, L. 2006. TT8 controls its own expression in a feedback regulation involving TTG1 and homologous MYB and bHLH factors, allowing a strong and cell-specific accumulation of flavonoids in *Arabidopsis* thaliana. Plant J. 46, 768-79.

Bernhardt, C., Lee, M.M., Gonzalez, A., Zhang, F., Lloyd, A. and Schiefelbein, J. 2003. The bHLH genes GLABRA3 (GL3) and ENHANCER OF GLABRA3 (EGL3) specify epidermal cell fate in the *Arabidopsis* root. Development, 130, 6431-39.

Bernhardt, C., Zhao, M., Gonzalez, A., Lloyd, A., and Schiefelbein, J. 2005. The bHLH genes GL3 and EGL3 participate in an intercellular regulatory circuit that controls cell patterning in the *Arabidopsis* root epidermis. Development 132(2): 291-298.

Borevitz, J. O., Xia, Y., Blount, J., Dixon, R. A. and Lamb, C. 2000. Activation tagging identifies a conserved MYB regulator of phenylpropanoid biosynthesis. Plant Cell, 12, 2383-2394.

Borovsky, Y., Oren-Shamir, M., Ovadia, R., De Jong, W. and Paran, I. 2004. The A locus that controls anthocyanin accumulation in pepper encodes a MYB transcription factor homologous to Anthocyanin2 of Petunia. Theor Appl Genet, 109: 23-29.

Brugliera, F., Barri-Rewell, G., Holton, T. A. and Mason, J. G. 1999. Isoloation and characterization of a flavonoid 3'-hydroxylase cDNA clone corresponding to the Ht1 locus of Petunia hybrida. Plant J., 19, 441-51.

Burr, F. A., Burr, B., SchefflerIb, B. E., Blewitt, M., Wienand, U. and Matza, E. C. 1996. The maize repressor-like gene intensifier1 shares homology with the r1/b1 multigene family of transcription factors and exhibits missplicing. Plant Cell, 8, 1249-1259.

Carey, C. C., Strahle, J. T., Selinger, D. A. and Chandler, V. 2004. Mutations in the pale aleurone color1 regulatory gene of the Zea mays anthocyanin pathway have distinct phenotype relative to the functionally similar Transparent Testa Glabra1 gene in *Arabidopsis* thaliana. Plant Cell, 16, 450-64.

Caro, E., Castellano, M.M., and Gutierrez, C. 2007. A chromatin link that couples cell division to root epidermis patterning in *Arabidopsis*. Nature 447(7141): 213-217.

Chandler, V. L., Radicella, J. P., Robbins, T. P., Chen, J. and Turks, D. 1989. Two regulatory genes of the maize anthocyanin pathway are homologous: isolation of b utilizing r genomic sequences. Plant Cell, 1, 1175-1183.

Cone, K. C., Burr, F. A. and Benjamin, B. 1986. Molecular analysis of the maize anthocyanin regulatory locus c1. Proc. Natl. Acad. Sci., 83, 9631-9635.

Czechowski T, Bari RP, Stitt M, Scheible WR, Udvardi MK. 2004. Real-time RT-PCR profiling of over 1400 *Arabidopsis* transcription factors: unprecedented sensitivity reveals novel root- and shoot-specific genes. Plant J 38: 366-379.

de Vetten, N., Quattrocchio, F., Mol, J., and Koes, R. 1997. The an11 locus controlling flower pigmentation in petunia encodes a novel WD-repeat protein conserved in yeast, plants, and animals. Genes Dev 11(11): 1422-1434.

Deboo, G. B., Albertsen, M. C. and Taylor, L. P. 1995. Flavonone 3-hydroxylase transcripts and flavonol accumulation are temporally coordinated in maize anthers. Plant J., 7, 703-713.

Deng, X.W., Matsui, M., Wei, N., Wagner, D., Chu, A.M., Feldmann, K.A., and Quail, P.H. 1992. COP1, an *Arabidopsis* regulatory gene, encodes a protein with both a zinc-binding motif and a G beta homologous domain. *Cell* 71(5): 791-801.

Di Cristina, M., Sessa, G., Dolan, L., Linstead, P., Baima, S., Ruberti, I., and Morelli, G. 1996. The *Arabidopsis* Athb-10 (GLABRA2) is an HD-Zip protein required for regulation of root hair development. Plant J 10(3): 393-402.

Downes, B.P., Stupar, R.M., Gingerich, D.J., and Vierstra, R.D. 2003. The HECT ubiquitin-protein ligase (UPL) family in *Arabidopsis*: UPL3 has a specific role in trichome development. *Plant J* 35(6): 729-742.

Edwards DR, Mahadevan LC. 1992. Protein synthesis inhibitors differentially superinduce c-fos and c-jun by three distinct mechanisms: lack of evidence for labile repressors. EMBO J 11: 2415-2424.

Esch, J.J., Chen, M., Sanders, M., Hillestad, M., Ndkium, S., Idelkope, B., Neizer, J., and Marks, M.D. 2003. A contradictory GLABRA3 allele helps define gene interactions controlling trichome development in *Arabidopsis*. Development 130(24): 5885-5894.

Feller A, Hernandez JM, Grotewold E. 2006. An ACT-like domain participates in the dimerization of several plant bHLH transcription factors. J Biol Chem 281: 28964 – 28974.

Galway, M.E., Masucci, J.D., Lloyd, A.M., Walbot, V., Davis, R.W., and Schiefelbein, J.W. 1994. The TTG gene is required to specify epidermal cell fate and cell patterning in the *Arabidopsis* root. *Dev Biol* 166(2): 740-754.

Goff, S. A., Cone, K. C. and Chandler, V. L. 1992. Functional analysis of the transcriptional activator encoded by the maize B gene: evidence for a direct functional interaction between two classes of regulatory proteins. Genes Dev., 6, 864-75.

Gray-Mitsumune, M., Molitor, E.K., Cukovic, D., Carlson, J.E., and Douglas, C.J. 1999. Developmentally regulated patterns of expression directed by poplar PAL promoters in transgenic tobacco and poplar. Plant Mol Biol 39(4): 657-669.

Hartmann, U., Sagasser, M., Mehrtens, F., Stracke, R. and Weisshaar, B. 2005. Differential combinatorial interactions of cis-acting elements recognized by

R2R3-MYB, BZIP, and BHLH factors control light-responsive and tissue-specific activation of phenylpropanoid biosynthesis genes. Plant Molecular Biology, 57, 155-71.

Hulskamp M, Misera S, Jurgens G. 1994. Genetic dissection of trichome cell development in *Arabidopsis*. Cell 76: 555-566.

Hulskamp, M. and Schnittger, A. 1998. Spatial regulation of trichome formation in *Arabidopsis* thaliana. Semin Cell Dev Biol 9(2): 213-220.

Hulskamp, M., Schnittger, A., and Folkers, U. 1999. Pattern formation and cell differentiation: trichomes in *Arabidopsis* as a genetic model system. Int Rev Cytol 186: 147-178.

Johnson, C.S., Kolevski, B., and Smyth, D.R. 2002. TRANSPARENT TESTA GLABRA2, a trichome and seed coat development gene of *Arabidopsis*, encodes a WRKY transcription factor. Plant Cell 14(6): 1359-1375.

Jorgensen, K., Rasmussen, A.V., Morant, M., Nielsen, A.H., Bjarnholt, N., Zagrobelny, M., Bak, S. and Moller, B.L. 2005. Metabolon formation and metabolic channeling in the biosynthesis of plant natural products. Curr. Opin. Plant Biol. 8, 280-291.

Karimi M, Inze D, Depicker A. 2002. GATEWAY vectors for Agrobacterium-mediated plant transformation. Trends Plant Sci 7: 193-195.

Kirik, V., Simon, M., Huelskamp, M., and Schiefelbein, J. 2004a. The ENHANCER OF TRY AND CPC1 gene acts redundantly with TRIPTYCHON and CAPRICE in trichome and root hair cell patterning in *Arabidopsis*. Dev Biol 268(2): 506-513.

Kirik, V., Simon, M., Wester, K., Schiefelbein, J., and Hulskamp, M. 2004b. ENHANCER of TRY and CPC 2 (ETC2) reveals redundancy in the region-specific control of trichome development of *Arabidopsis*. Plant Mol Biol 55(3): 389-398.

Koornneef, M. 1981. The complex syndrome of ttg mutants. Arabid. Inf. Serv. 18, 45-51.

Koornneef, M., Dellaert, L. and van der Veen, J. 1982. EMS- and radiation-induced mutation frequencies at individual loci in *Arabidopsis* thaliana (L.) Heynh. Mutat. Res. 93, 109-123.

Koshino-Kimura, Y., Wada, T., Tachibana, T., Tsugeki, R., Ishiguro, S., and Okada, K. 2005. Regulation of CAPRICE transcription by MYB proteins for root epidermis differentiation in *Arabidopsis*. Plant Cell Physiol 46(6): 817-826.

Larkin, J.C., Brown, M.L., and Schiefelbein, J. 2003. How do cells know what they want to be when they grow up? Lessons from epidermal patterning in *Arabidopsis*. Annu Rev Plant Biol 54: 403-430.

Larkin, J.C., Marks, M.D., Nadeau, J., and Sack, F. 1997. Epidermal cell fate and patterning in leaves. Plant Cell 9(7): 1109-1120.

Larkin JC, Oppenheimer DG, Pollock S, Marks MD. 1993. *Arabidopsis* GLABROUS1 gene requires downstream sequences for function. Plant Cell 5: 1739-1748.

Larkin, J.C., Young, N., Prigge, M., and Marks, M.D. 1996. The control of trichome spacing and number in *Arabidopsis*. Development 122(3): 997-1005.

Lee, M.M. and Schiefelbein, J. 1999. WEREWOLF, a MYB-related protein in *Arabidopsis*, is a position-dependent regulator of epidermal cell patterning. Cell, 99, 473–83.

Lee, M.M. and Schiefelbein, J. 2001. Developmentally distinct MYB genes encode functionally equivalent proteins in *Arabidopsis*. Development 128(9): 1539-1546.

Lee, M.M. and Schiefelbein, J. 2002. Cell pattern in the *Arabidopsis* root epidermis determined by lateral inhibition with feedback. Plant Cell 14(3): 611-618.

Lepiniec, L., Debeaujon, I., Routaboul, J., Baudry, A., Pourcel, L., Nesi, N. and Caboche, M. 2006. Genetics and biochemistry of seed flavonoids. Annu. Rev. Plant Biol., 57, 405-30.

Lin, X., Kaul, S., Rounsley, S., Shea, T.P., Benito, M.I., Town, C.D., Fujii, C.Y., Mason, T., Bowman, C.L., Barnstead, M., Feldblyum, T.V., Buell, C.R., Ketchum, K.A., Lee, J., Ronning, C.M., Koo, H.L., Moffat, K.S., Cronin, L.A., Shen, M., Pai, G., Van Aken, S., Umayam, L., Tallon, L.J., Gill, J.E., Adams, M.D., Carrera, A.J., Creasy, T.H., Goodman, H.M., Somerville, C.R., Copenhaver, G.P., Preuss, D., Nierman, W.C., White, O., Eisen, J.A., Salzberg, S.L., Fraser, C.M., and Venter, J.C. 1999. Sequence and analysis of chromosome 2 of the plant *Arabidopsis* thaliana. *Nature* 402(6763): 761-768.

Lloyd, A.M., Walbot, V., and Davis, R.W. 1992. *Arabidopsis* and Nicotiana anthocyanin production activated by maize regulators R and C1. *Science* 258(5089): 1773-1775.

Lloyd AM, Davis RW. 1994. Functional expression of the yeast FLP/FRT site-specific recombination system in Nicotiana tabacum. Mol Gen Genet 242: 653-657.

Lloyd AM, Schena M, Walbot V, Davis RW. 1994. Epidermal cell fate determination in *Arabidopsis*: Patterns defined by a steroid-inducible regulator. Science 266: 436-439.

Ludwig, S. R., Habera, L. F., Dellaporta, S. L. and Wessler, S. R. 1989. Lc, a member of the maize r gene family responsible for tissue-specific anthocyanin production, encodes a protein similar to transcriptional activators and contains the myc-homology region. Proc. Natl. Acad. Sci., 86, 7092-7096.

Marks, M.D. 1997. Molecular Genetic Analysis of Trichome Development in *Arabidopsis*. Annu Rev Plant Physiol Plant Mol Biol 48: 137-163.

Marks MD, Esch JJ. 2003. Initiating inhibition. Control of epidermal cell patterning in plants. EMBO Rep 4: 24-25.

Masucci, J.D., Rerie, W.G., Foreman, D.R., Zhang, M., Galway, M.E., Marks, M.D., and Schiefelbein, J.W. 1996. The homeobox gene GLABRA2 is required for position-dependent cell differentiation in the root epidermis of *Arabidopsis* thaliana. Development 122(4): 1253-1260.

Martin, C., Prescott, A., Mackay, S., Bartlett, J. and Vrijlandt, E. 1991. Control of anthocyanin biosynthesis in flowers of Antirrhinurn majus. Plant J., 1, 37-49.

Mayer, K. Schuller, C. Wambutt, R. Murphy, G. Volckaert, G. Pohl, T. Dusterhoft, A. Stiekema, W. Entian, K.D. Terryn, N. Harris, B. Ansorge, W. Brandt, P. Grivell, L. Rieger, M. Weichselgartner, M. de Simone, V. Obermaier, B. Mache, R.

Muller, M. Kreis, M. Delseny, M. Puigdomenech, P. Watson, M. Schmidtheini, T. Reichert, B. Portatelle, D. Perez-Alonso, M. Boutry, M. Bancroft, I. Vos, P. Hoheisel, J. Zimmermann, W. Wedler, H. Ridley, P. Langham, S.A. McCullagh, B. Bilham, L. Robben, J. Van der Schueren, J. Grymonprez, B. Chuang, Y.J. Vandenbussche, F. Braeken, M. Weltjens, I. Voet, M. Bastiaens, I. Aert, R. Defoor, E. Weitzenegger, T. Bothe, G. Ramsperger, U. Hilbert, H. Braun, M. Holzer, E. Brandt, A. Peters, S. van Staveren, M. Dirske, W. Mooijman, P. Klein Lankhorst, R. Rose, M. Hauf, J. Kotter, P. Berneiser, S. Hempel, S. Feldpausch, M. Lamberth, S. Van den Daele, H. De Keyser, A. Buysshaert, C. Gielen, J. Villarroel, R. De Clercq, R. Van Montagu, M. Rogers, J. Cronin, A. Quail, M. Bray-Allen, S. Clark, L. Doggett, J. Hall, S. Kay, M. Lennard, N. McLay, K. Mayes, R. Pettett, A. Rajandream, M.A. Lyne, M. Benes, V. Rechmann, S. Borkova, D. Blocker, H. Scharfe, M. Grimm, M. Lohnert, T.H. Dose, S. de Haan, M. Maarse, A. Schafer, M. Muller-Auer, S. Gabel, C. Fuchs, M. Fartmann, B. Granderath, K. Dauner, D. Herzl, A. Neumann, S. Argiriou, A. Vitale, D. Liguori, R. Piravandi, E. Massenet, O. Quigley, F. Clabauld, G. Mundlein, A. Felber, R. Schnabl, S. Hiller, R. Schmidt, W. Lecharny, A. Aubourg, S. Chefdor, F. Cooke, R. Berger, C. Montfort, A. Casacuberta, E. Gibbons, T. Weber, N. Vandenbol, M. Bargues, M. Terol, J. Torres, A. Perez-Perez, A. Purnelle, B. Bent, E. Johnson, S. Tacon, D. Jesse, T. Heijnen, L. Schwarz, S. Scholler, P. Heber, S. Francs, P. Bielke, C. Frishman, D. Haase, D. Lemcke, K. Mewes, H.W. Stocker, S. Zaccaria, P. Bevan, M. Wilson, R.K. de la Bastide, M. Habermann, K. Parnell, L. Dedhia,

N. Gnoj, L. Schutz, K. Huang, E. Spiegel, L. Sehkon, M. Murray, J. Sheet, P. Cordes, M. Abu-Threideh, J. Stoneking, T. Kalicki, J. Graves, T. Harmon, G. Edwards, J. Latreille, P. Courtney, L. Cloud, J. Abbott, A. Scott, K. Johnson, D. Minx, P. Bentley, D. Fulton, B. Miller, N. Greco, T. Kemp, K. Kramer, J. Fulton, L. Mardis, E. Dante, M. Pepin, K. Hillier, L. Nelson, J. Spieth, J. Ryan, E. Andrews, S. Geisel, C. Layman, D. Du, H. Ali, J. Berghoff, A. Jones, K. Drone, K. Cotton, M. Joshu, C. Antonoiu, B. Zidanic, M. Strong, C. Sun, H. Lamar, B. Yordan, C. Ma, P. Zhong, J. Preston, R. Vil, D. Shekher, M. Matero, A. Shah, R. Swaby, I.K. O'Shaughnessy, A. Rodriguez, M. Hoffmann, J. Till, S. Granat, S. Shohdy, N. Hasegawa, A. Hameed, A. Lodhi, M. Johnson, A. Chen, E. Marra, M. Martienssen, R. and McCombie, W.R. 1999. Sequence and analysis of chromosome 4 of the plant *Arabidopsis* thaliana. *Nature* 402(6763): 769-777.

Meinhardt, H. 1994. Biological pattern formation: new observations provide support for theoretical predictions. Bioessays 16(9): 627-632.

Meinhardt H, Gierer A (1974) Applications of a theory of biological pattern formation based on lateral inhibition. J Cell Sci 15: 321-346.

Meinhardt, H. and Gierer, A. 2000. Pattern formation by local self-activation and lateral inhibition. Bioessays 22(8): 753-760.

Morita, Y., Saitoh, M., Hoshino, A., Nitasaka, E. and Iida, S. 2006. Isolation of cDNAs for R2R3-MYB, bHLH and WDR transcriptional regulators and identification of c and ca mutations conferring white flowers in the Japanese Morning Glory. Plant Cell Physiology, 47, 457-470.

Neer, E.J., Schmidt, C.J., Nambudripad, R., and Smith, T.F. 1994. The ancient regulatory-protein family of WD-repeat proteins. *Nature* 371(6495): 297-300.

Nemeth, K., Salchert, K., Putnoky, P., Bhalerao, R., Koncz-Kalman, Z., Stankovic-Stangeland, B., Bako, L., Mathur, J., Okresz, L., Stabel, S., Geigenberger, P., Stitt, M., Redei, G.P., Schell, J., and Koncz, C. 1998. Pleiotropic control of glucose and hormone responses by PRL1, a nuclear WD protein, in *Arabidopsis*. *Genes Dev* 12(19): 3059-3073.

Nesi, N., Debeaujon, I., Jond, C., Pelletier, G., Caboche, M. and Lepiniec, L. 2000. The TT8 gene encodes a basic helix-loop-helix domain protein required for expression of DFR and BAN genes in *Arabidopsis* siliques. Plant Cell, 12, 1863-78.

Nesi, N., Jond, C., Debeaujon, I., Caboche, M. and Lepiniec, L. 2001. The *Arabidopsis* TT2 gene encodes an R2R3 MYB domain protein that acts as a key determinant for proanthocyanidin accumulation in developing seed. Plant Cell, 13, 2099-114.

Ohashi, Y., Oka, A., Rodrigues-Pousada, R., Possenti, M., Ruberti, I., Morelli, G., and Aoyama, T. 2003. Modulation of phospholipid signaling by GLABRA2 in root-hair pattern formation. Science 300(5624): 1427-1430.

Ohashi, Y., Oka, A., Ruberti, I., Morelli, G., and Aoyama, T. 2002. Entopically additive expression of GLABRA2 alters the frequency and spacing of trichome initiation. Plant J 29(3): 359-369.

Oppenheimer, D.G., Herman, P.L., Sivakumaran, S., Esch, J., and Marks, M.D. 1991. A myb gene required for leaf trichome differentiation in *Arabidopsis* is expressed in stipules. Cell 67(3): 483-493.

Payne, T., Clement, J., Arnold, D., and Lloyd, A. 1999. Heterologous myb genes distinct from GL1 enhance trichome production when overexpressed in Nicotiana tabacum. Development 126(4): 671-682.

Payne, C.T., Zhang, F., and Lloyd, A.M. 2000. GL3 encodes a bHLH protein that regulates trichome development in arabidopsis through interaction with GL1 and TTG1. Genetics 156(3): 1349-1362.

Paz-Ares, J., Ghosal, D., Wienand, U., Peterson, P. A. and Saedler, H. 1987. The regulatory c1 locus of Zea mays encodes a protein with homology to myb proto-oncogene products and with structural similarities to transcription factors. EMBO J., 6, 3553-58.

Pelletier, M. K., Murrell, J. R. and Winkel-Shirley, B. 1997. Characterization of flavonol synthase and leucoanthocyanidin dioxygenase genes in *Arabidopsis*. Plant Physiol., 113, 1437-1445.

Pelletier, M. K. and Winkel-Shirley, B. 1996. Analysis of Flavanone 3-Hydroxylase in *Arabidopsis* Seedlings. Plant Physiol., 111, 339-345.

Pelletier, M. K., Burbulis, I. E. and Winkel-Shirley, B. 1999. Disruption of specific flavonoid genes enhances the accumulation of flavonoid end-products in *Arabidopsis* seedlings. Plant Molecular Biology, 40, 45-54.

Perazza, D., Vachon, G., and Herzog, M. 1998. Gibberellins promote trichome formation by Up-regulating GLABROUS1 in arabidopsis. *Plant Physiol* 117(2): 375-383.

Pesch, M. and Hulskamp, M. 2004. Creating a two-dimensional pattern de novo during *Arabidopsis* trichome and root hair initiation. Curr Opin Genet Dev 14(4): 422-427.

Piazza, P., Procissi, A., Jenkins, G. I. and Tonelli, C. 2002. Members of the c1/pl1 regulatory gene family mediate the response of maize aleurone and mesocotyl to different light qualities and cytokinins. Plant Physiol., 128, 1077-1086.

Quattrocchio, F., Wing, J., van der Woude, K., Souer, E., de Vetten, N., Mol, J. and Koes, R. 1999. Molecular analysis of the Anthocyanin2 gene of Petunia and its role in the evolution of flower color. Plant Cell, 11, 1433-44.

Quattrocchio, F., Wing, J. F., Leppen, H. T. C., Mol, J. N. M. and Koes, R. E. 1993. Regulatory genes controlling anthocyanin pigmentation are functionally conserved among plant species and have distinct sets of target genes. Plant Cell, 5, 1497-1512.

Ramsay, N.A. and Glover, B.J. 2005. MYB-bHLH-WD40 protein complex and the evolution of cellular diversity. *Trends Plant Sci* 10(2): 63-70.

Rerie, W.G., Feldmann, K.A., and Marks, M.D. 1994. The GLABRA2 gene encodes a homeo domain protein required for normal trichome development in *Arabidopsis*. Genes Dev 8(12): 1388-1399.

Roth MB, Zahler AM, Stolk JA. 1991. A conserved family of nuclear phosphoproteins localized to sites of polymerase II transcription. J Cell Biol 115:587–596.

Ryu, K.H., Kang, Y.H., Park, Y.H., Hwang, I., Schiefelbein, J., and Lee, M.M. 2005. The WEREWOLF MYB protein directly regulates CAPRICE transcription during cell

fate specification in the *Arabidopsis* root epidermis. Development 132(21): 4765-4775.

Sablowski, R.W. and Meyerowitz, E.M. 1998. A homolog of NO APICAL MERISTEM is an immediate target of the floral homeotic genes APETALA3/PISTILLATA. Cell 92(1): 93-103.

Salanoubat, M. Lemcke, K. Rieger, M. Ansorge, W. Unseld, M. Fartmann, B. Valle, G. Blocker, H. Perez-Alonso, M. Obermaier, B. Delseny, M. Boutry, M. Grivell, L.A. Mache, R. Puigdomenech, P. De Simone, V. Choisne, N. Artiguenave, F. Robert, C. Brottier, P. Wincker, P. Cattolico, L. Weissenbach, J. Saurin, W. Quetier, F. Schafer, M. Muller-Auer, S. Gabel, C. Fuchs, M. Benes, V. Wurmbach, E. Drzonek, H. Erfle, H. Jordan, N. Bangert, S. Wiedelmann, R. Kranz, H. Voss, H. Holland, R. Brandt, P. Nyakatura, G. Vezzi, A. D'Angelo, M. Pallavicini, A. Toppo, S. Simionati, B. Conrad, A. Hornischer, K. Kauer, G. Lohnert, T.H. Nordsiek, G. Reichelt, J. Scharfe, M. Schon, O. Bargues, M. Terol, J. Climent, J. Navarro, P. Collado, C. Perez-Perez, A. Ottenwalder, B. Duchemin, D. Cooke, R. Laudie, M. Berger-Llauro, C. Purnelle, B. Masuy, D. de Haan, M. Maarse, A.C. Alcaraz, J.P. Cottet, A. Casacuberta, E. Monfort, A. Argiriou, A. flores, M. Liguori, R. Vitale, D. Mannhaupt, G. Haase, D. Schoof, H. Rudd, S. Zaccaria, P. Mewes, H.W. Mayer, K.F. Kaul, S. Town, C.D. Koo, H.L. Tallon, L.J. Jenkins, J. Rooney, T. Rizzo, M. Walts, A. Utterback, T. Fujii, C.Y. Shea, T.P. Creasy, T.H. Haas, B. Maiti, R. Wu, D. Peterson, J. Van Aken, S. Pai, G. Militscher, J. Sellers, P. Gill, J.E. Feldblyum, T.V. Preuss, D. Lin, X. Nierman,

W.C. Salzberg, S.L. White, O. Venter, J.C. Fraser, C.M. Kaneko, T. Nakamura, Y. Sato, S. Kato, T. Asamizu, E. Sasamoto, S. Kimura, T. Idesawa, K. Kawashima, K. Kishida, Y. Kiyokawa, C. Kohara, M. Matsumoto, M. Matsuno, A. Muraki, A. Nakayama, S. Nakazaki, N. Shinpo, S. Takeuchi, C. Wada, T. Watanabe, A. Yamada, M. Yasuda, M. and Tabata, S. 2000. Sequence and analysis of chromosome 3 of the plant *Arabidopsis* thaliana. *Nature* 408(6814): 820-822.

Schellmann S, Hulskamp M. 2005. Epidermal differentiation: trichomes in *Arabidopsis* as a model system. Int. J. Dev. Biol.: 579-584.

Schellmann, S., Schnittger, A., Kirik, V., Wada, T., Okada, K., Beermann, A., Thumfahrt, J., Jurgens, G., and Hulskamp, M. 2002. TRIPTYCHON and CAPRICE mediate lateral inhibition during trichome and root hair patterning in *Arabidopsis*. EMBO J 21(19): 5036-5046.

Schnittger, A., Folkers, U., Schwab, B., Jurgens, G., and Hulskamp, M. 1999. Generation of a spacing pattern: the role of triptychon in trichome patterning in *Arabidopsis*. Plant Cell 11(6): 1105-1116.

Schwinn, K., Venail, J., Shang, Y., Mackay, S., Alm, V., Butelli, E., Oyama, R., Bailey, P., Davies, K. and Martin, C. 2006. A small family of MYB-regulatory genes controls floral pigmentation intensity and patterning in the genus Antirrhinum. Plant Cell, 18, 831-851.

Serna, L. and Martin, C. 2006. Trichomes: different regulatory networks lead to convergent structures. Trends in Plant Science, 11, 274-80.

Solfanelli, C., Poggi, A., Loreti, E., Alpi, A. and Perata, P. 2006. Sucrose-specific induction of the anthocyanin biosynthetic pathway in *Arabidopsis*. Plant Physiol., 140, 637-646.

Spelt, C., Quattrocchio, F., Mol, J. N. and Koes, R. 2000. Anthocyanin1 of petunia encodes a basic helix-loop-helix protein that directly activates transcription of structural anthocyanin genes. Plant Cell, 12, 1619-32.

Stracke, R., Werber, M. and Weisshaar, B. 2001. The R2R3-MYB gene family in *Arabidopsis* thaliana. Current Opinion in Plant Biology, 4, 447-456.

Szymanski D, Lloyd A, Marks MD. 2000. Progress in the molecular genetic analysis of trichome initiation and morhpogenesis in *Arabidopsis*. Trends Plant Sci. 5: 214-219.

Szymanski, D.B., Jilk, R.A., Pollock, S.M., and Marks, M.D. 1998. Control of GL2 expression in *Arabidopsis* leaves and trichomes. Development 125(7): 1161-1171.

Tabata, S. Kaneko, T. Nakamura, Y. Kotani, H. Kato, T. Asamizu, E. Miyajima, N. Sasamoto, S. Kimura, T. Hosouchi, T. Kawashima, K. Kohara, M. Matsumoto, M. Matsuno, A. Muraki, A. Nakayama, S. Nakazaki, N. Naruo, K. Okumura, S. Shinpo, S. Takeuchi, C. Wada, T. Watanabe, A. Yamada, M. Yasuda, M. Sato, S. de la Bastide, M. Huang, E. Spiegel, L. Gnoj, L. O'Shaughnessy, A. Preston, R. Habermann, K. Murray, J. Johnson, D. Rohlfing, T. Nelson, J. Stoneking, T. Pepin, K. Spieth, J. Sekhon, M. Armstrong, J. Becker, M. Belter, E. Cordum, H. Cordes, M. Courtney, L. Courtney, W. Dante, M. Du, H. Edwards, J. Fryman, J. Haakensen, B. Lamar, E. Latreille, P. Leonard, S. Meyer, R. Mulvaney, E.

Ozersky, P. Riley, A. Strowmatt, C. Wagner-McPherson, C. Wollam, A. Yoakum, M. Bell, M. Dedhia, N. Parnell, L. Shah, R. Rodriguez, M. See, L.H. Vil, D. Baker, J. Kirchoff, K. Toth, K. King, L. Bahret, A. Miller, B. Marra, M. Martienssen, R. McCombie, W.R. Wilson, R.K. Murphy, G. Bancroft, I. Volckaert, G. Wambutt, R. Dusterhoft, A. Stiekema, W. Pohl, T. Entian, K.D. Terryn, N. Hartley, N. Bent, E. Johnson, S. Langham, S.A. McCullagh, B. Robben, J. Grymonprez, B. Zimmermann, W. Ramsperger, U. Wedler, H. Balke, K. Wedler, E. Peters, S. van Staveren, M. Dirkse, W. Mooijman, P. Lankhorst, R.K. Weitzenegger, T. Bothe, G. Rose, M. Hauf, J. Berneiser, S. Hempel, S. Feldpausch, M. Lamberth, S. Villarroel, R. Gielen, J. Ardiles, W. Bents, O. Lemcke, K. Kolesov, G. Mayer, K. Rudd, S. Schoof, H. Schueller, C. Zaccaria, P. Mewes, H.W. Bevan, M. and Fransz, P. 2000. Sequence and analysis of chromosome 5 of the plant *Arabidopsis* thaliana. *Nature* 408(6814): 823-826.

Taylor, L. P. and Briggs, W. R. 1990. Genetic regulation and photocontrol of anthocyanin accumulation in maize seedlings. Plant Cell, 2, 115-127.

Teng, S., Keurentjes, J., Bentsink, L., Koornneef, M. and Smeekens, S. 2005. Sucrose-specific induction of anthocyanin biosynthesis in *Arabidopsis* requires the MYB75/PAP1 gene. Plant Physiol., 139, 1840-52.

Theologis, A., Ecker, J.R., Palm, C.J., Federspiel, N.A., Kaul, S., White, O., Alonso, J., Altafi, H., Araujo, R., Bowman, C.L., Brooks, S.Y., Buehler, E., Chan, A., Chao, Q., Chen, H., Cheuk, R.F., Chin, C.W., Chung, M.K., Conn, L., Conway, A.B., Conway, A.R., Creasy, T.H., Dewar, K., Dunn, P., Etgu, P., Feldblyum, T.V.,

Feng, J., Fong, B., Fujii, C.Y., Gill, J.E., Goldsmith, A.D., Haas, B., Hansen, N.F., Hughes, B., Huizar, L., Hunter, J.L., Jenkins, J., Johnson-Hopson, C., Khan, S., Khaykin, E., Kim, C.J., Koo, H.L., Kremenetskaia, I., Kurtz, D.B., Kwan, A., Lam, B., Langin-Hooper, S., Lee, A., Lee, J.M., Lenz, C.A., Li, J.H., Li, Y., Lin, X., Liu, S.X., Liu, Z.A., Luros, J.S., Maiti, R., Marziali, A., Militscher, J., Miranda, M., Nguyen, M., Nierman, W.C., Osborne, B.I., Pai, G., Peterson, J., Pham, P.K., Rizzo, M., Rooney, T., Rowley, D., Sakano, H., Salzberg, S.L., Schwartz, J.R., Shinn, P., Southwick, A.M., Sun, H., Tallon, L.J., Tambunga, G., Toriumi, M.J., Town, C.D., Utterback, T., Van Aken, S., Vaysberg, M., Vysotskaia, V.S., Walker, M., Wu, D., Yu, G., Fraser, C.M., Venter, J.C., and Davis, R.W. 2000. Sequence and analysis of chromosome 1 of the plant *Arabidopsis* thaliana. *Nature* 408(6814): 816-820.

Tohge, T., Nishiyama, Y., Hirai, M. Y., Yano, M., Nakajima, J., Awazuhara, M., Inoue, E., Takahashi, H., Goodenowe, D. B., Kitayama, M. et al. 2005. Functional genomics by integrated analysis of metabolome and transcriptome of *Arabidopsis* plants over-expressing an MYB transcription factor. Plant J., 42, 218-235.

Torii, K.U., McNellis, T.W., and Deng, X.W. 1998. Functional dissection of *Arabidopsis* COP1 reveals specific roles of its three structural modules in light control of seedling development. *EMBO J* 17(19): 5577-5587.

Traw, M.B. and Bergelson, J. 2003. Interactive effects of jasmonic acid, salicylic acid, and gibberellin on induction of trichomes in *Arabidopsis*. *Plant Physiol* 133(3): 1367-1375.

Wada, T., Kurata, T., Tominaga, R., Koshino-Kimura, Y., Tachibana, T., Goto, K., Marks, M.D., Shimura, Y., and Okada, K. 2002. Role of a positive regulator of root hair development, CAPRICE, in *Arabidopsis* root epidermal cell differentiation. Development 129(23): 5409-5419.

Wada, T., Tachibana, T., Shimura, Y., and Okada, K. 1997. Epidermal cell differentiation in *Arabidopsis* determined by a Myb homolog, CPC. Science 277(5329): 1113-1116.

Walker, A.R., Davison, P.A., Bolognesi-Winfield, A.C., James, C.M., Srinivasan, N., Blundell, T.L., Esch, J.J., Marks, M.D., and Gray, J.C. 1999. The TRANSPARENT TESTA GLABRA1 locus, which regulates trichome differentiation and anthocyanin biosynthesis in *Arabidopsis*, encodes a WD40 repeat protein. Plant Cell 11(7): 1337-1350.

Weiss, E.R., Osawa, S., Shi, W., and Dickerson, C.D. 1994. Effects of carboxyl-terminal truncation on the stability and G protein-coupling activity of bovine rhodopsin. *Biochemistry* 33(24): 7587-7593.

Winkel-Shirley, B., Kubasek, W. L., Storz, G., Bruggemann, E., Koornneef, M., Ausubel, F. M. and Goodman, H. M. 1995. Analysis of *Arabidopsis* mutants deficient in flavonoid biosynthesis. Plant J., 8, 659-71.

Winkel-Shirley, B. 2001. Flavonoid biosynthesis. A colorful model for genetics, biochemistry, cell biology, and biotechnology. Plant Physiol., 126, 485-93.

Zhang, F., Gonzalez, A., Zhao, M., Payne, C.T., and Lloyd, A. 2003. A network of redundant bHLH proteins functions in all TTG1-dependent pathways of *Arabidopsis*. Development 130(20): 4859-4869.

Zimmermann, I. M., Heim, M. A., Weisshaar, B. and Uhrig, J. F. 2004. Comprehensive identification of *Arabidopsis* thaliana MYB transcription factors interacting with R/B-like BHLH proteins. Plant J., 40, 22-34.

Vita

Mingzhe Zhao was born in Shenyang, Liaoning Province of People's Republic of China on May 27th, 1973, the son of Changhai Zhao and Yushu Zhao. After completing high school at Shenyang No.2 high school (Shenyang) in 1992, he entered Jilin University (Changchun, Jilin Province of China), where he received a degree of Bachelor of Science in Molecular biology in July 1996. He then continued his graduate study in the Department of Biochemistry and Molecular Biology at Peking University for three years and was awarded a degree of Master of Science. In the fall of 1999, he entered the graduate program of Molecular Cellular and Developmental Biology at the University of Texas at Austin.

Permanent address: 12129 Bellaire Blvd. Houston, TX 77072

This dissertation was typed by the author.